British Astronomical Association

Mercury & Venus Section Newsletter

Director: Dr Paul G. Abel

Messenger

No. 15, August 2024.

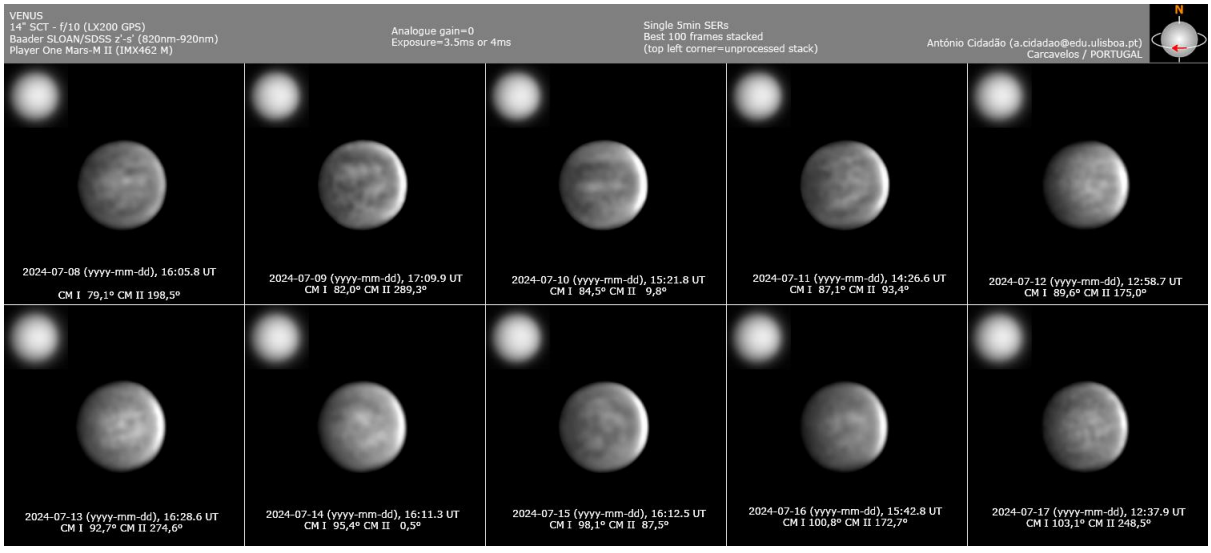

A set of Venus observations by Antonio Cidadao, taken on 8th – 12th July 2024

Contents

From the Director

Dear Members,

I hope this newsletter finds you all well and that you are enjoying the summer months which have seen some clear skies and better weather conditions. It is a pleasure to send you the 15th issue of Messenger, and in this issue we have two contributions: Chris Hooker provides and excellent write up of his results obtained in observing the ion tail of Mercury in March 2024. The second article is by Martin Lewis who has produced a splendid article on measuring the signal to noise ratio in night side images of Venus. I'm sure you will find both of these articles of great interest- they really do represent the cutting edge of observational research which the Section is carrying out!

Venus has now returned to the evening sky – currently it is rather low down, and the best way to observe it is during the daytime as I have done recently. This kind of observation requires real care: setting circles must be used and the planet is still close to the sun and if the sun is viewed through the telescope or binoculars even momentarily, instant blindness will result. So, if you are in any doubt it will be best to observe the planet when the sun has set. For the next few months this will require a clear western horizon.

Venus has been in the news again in the last few months: there have been further detections of phosphine and ammonia in the atmosphere of Venus. On Earth, phosphine and ammonia can be biomarkers and a number of scientists think these recent detections (along with those detected in 2020) might be being produced by some sort of microbial life in the atmosphere of Venus. I remain deeply sceptical about that, but it is now becoming quite hard to think of mechanisms which could produce these results in the quantities observed.

By the end of the end of the year, Venus will be a splendid evening target- please do go out and observe it and as ever, send me your observations as soon as you can. It is important we keep a watchful eye on bother our inner neighbours!

Clear Skies,

Paul G. Abel,
Director of the BAA Mercury & Venus Section

From the Mercury Coordinator

In May and early June, the western elongation of Mercury was favourable for observers in the northern hemisphere but less so in the south. However, the Section received images from observers both north and south of the equator. Here is a selection in chronological order:

22nd May from Clyde Foster in Namibia:

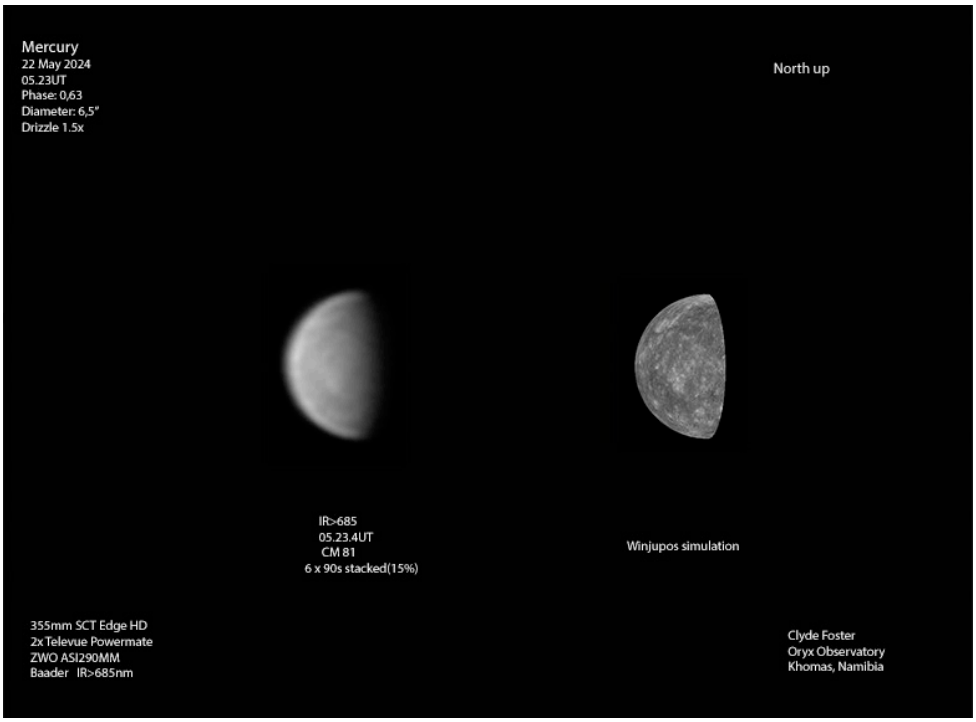

25th May from Frank Melillo in New York state:

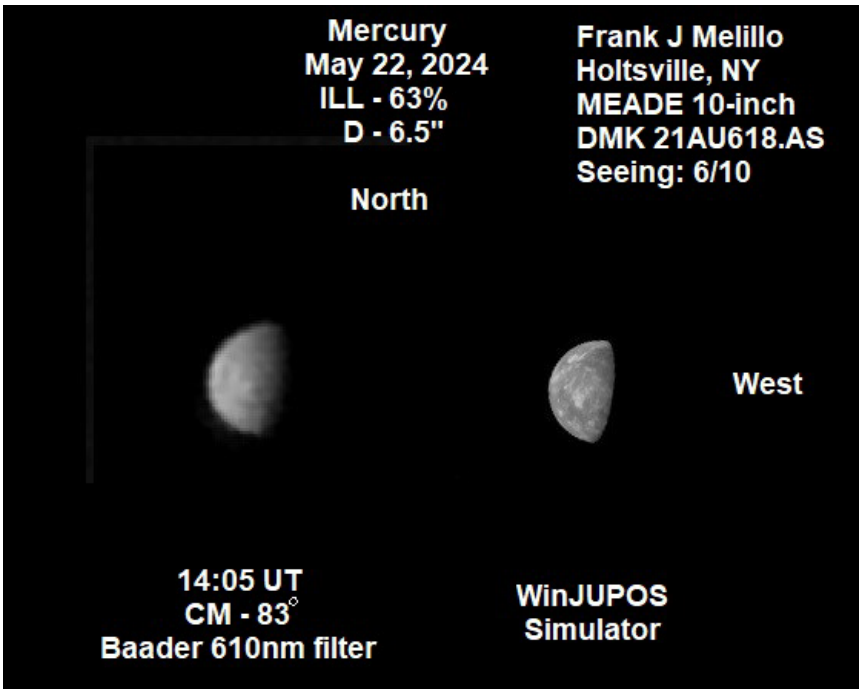

2nd June from Martin Lewis in St Albans, UK:

2nd June from Ron Palgrave in Stanley, UK

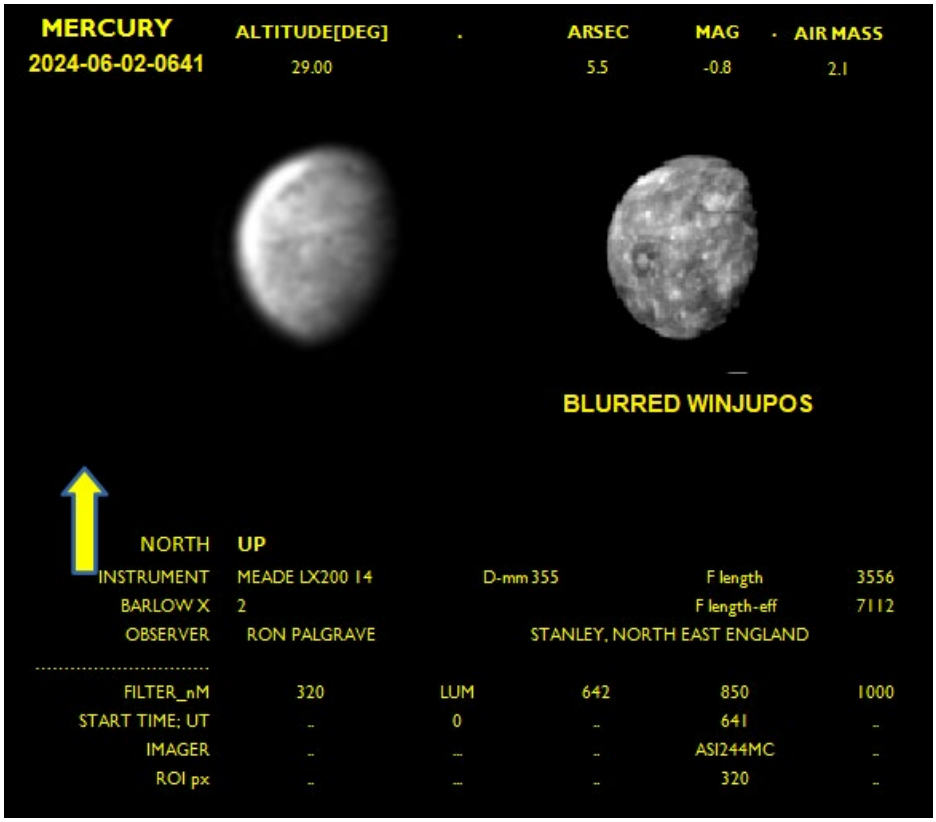

5th June from Chris Hooker in Didcot, UK:

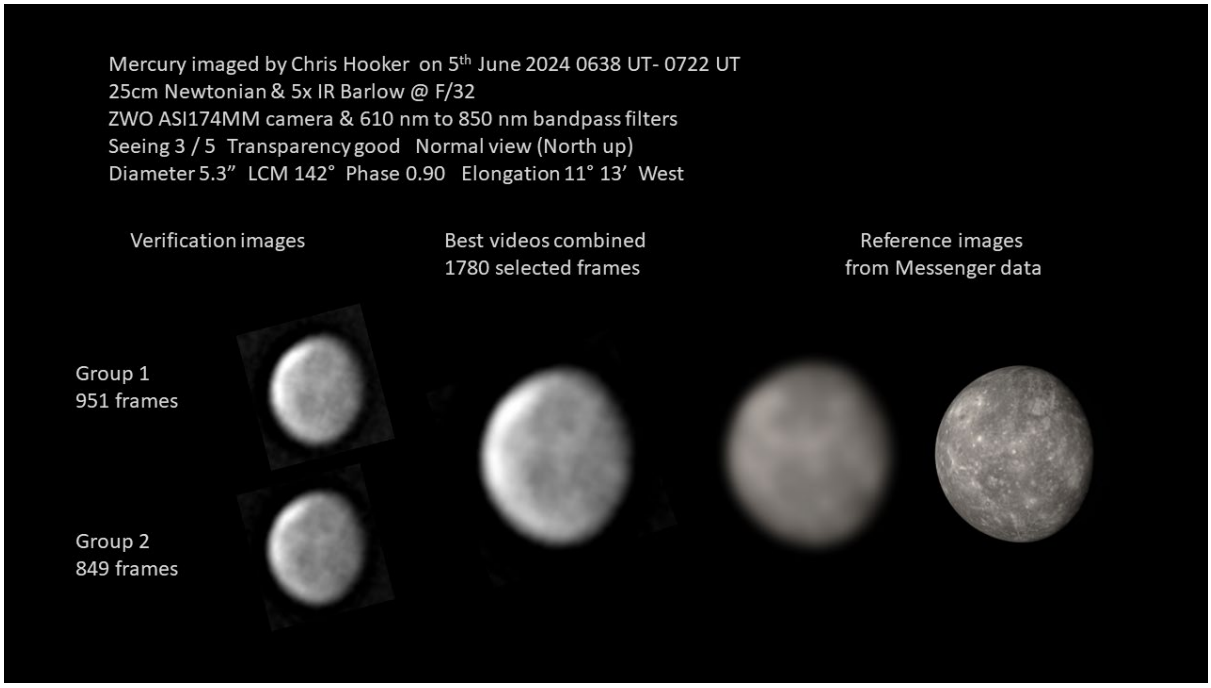

6th June from Luigi Morrone in Agerola, Italy:

Thanks to all the contributors for sending in their images.

Forthcoming events

Mercury passed through superior conjunction on the 14th of June. After that it appeared in the evening sky, but because of the low inclination of the ecliptic, it was very low in the WNW after sunset. Mercury and Venus were close together on the morning of the 17th of June, but at only three degrees east of the Sun this conjunction was not observable.

Although the chances for evening observation during the summer were limited, Mercury was high in the sky during the daytime, giving opportunities for imaging during the first three weeks of July. The British weather, alas, was not cooperative. At the time of writing Mercury has just passed greatest eastern elongation. It reaches 49 degrees altitude when due south but has faded to magnitude 0.5, so it will be hard to locate in the daytime sky and too low in the evening twilight. On the 14th of August it will be at inferior conjunction and will remain faint and hard to locate until early in September. The western elongation in September will again be favourable for northern hemisphere observers, with a chance for imagers to record the planet during its crescent phases. Anyone attempting to locate and image Mercury in daytime should take precautions as set out in the Mercury Observing Guide, which can be downloaded from the Section web page by BAA members (requires a login). Please send any images and other observations to me or to the Section Director.

During the previous eastern elongation in March, I was able to image Mercury's sodium tail in the evening sky. The window of opportunity for this was roughly ten days in length, and naturally the British weather made observing impossible on half of them. Nevertheless, several images were obtained showing a well-developed tail, and elsewhere in this issue is a report of these observations and some analysis of them.

At the start of May I was made aware of another image of the tail, captured by BAA member Mel Gigg from Witney. He used a Canon DSLR with a 300 mm F/2.8 lens and a sodium-line filter, and recorded the tail at 19:04 UT on the 29th of March:

Mercury's altitude at the time was slightly more than 2 degrees. The star close to Mercury at the 2 o'clock position is HIP7198, which at the time was 8.7 arc minutes from the planet. The part of the tail that is clearly visible extends about 50% further than that distance, or 13 arc minutes.

Chris Hooker

Mercury Co-ordinator

Venus in 2024-2025

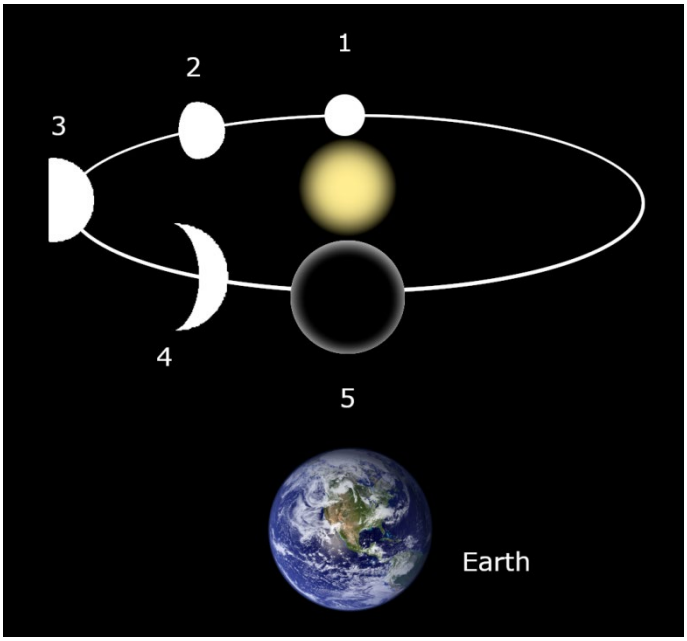

Figure 1: The orbit of Venus from superior conjunction to inferior conjunction in 2024-25

Date	Event	Position
2024 June 04	Superior conjunction: Venus returns to the evening sky and this marks the start of the 2024 – 2025 eastern elongation	1
2024 June – 2025 January 12	Venus is now in the evening sky, the planet will get higher in the autumn/winter sky and the phase of the planet will decrease as the planet moves towards us.	2-3
2025 January 12	Venus is at theoretical dichotomy (50% illuminated) and high in the evening sky.	3
2025 February 07	Venus reaches its highest altitude in the evening sky.	3-4
2025 February 16	Venus is at greatest brilliance on this day	4-5
2025 February 16 – 2025 March 23	Venus continues to move towards the earth and the apparent diameter of the planet increases while phase continues as a waning crescent.	4-5
2025 March 23	Venus reaches inferior conjunction. The planet is effectively between the sun and the earth- this marks the end of the 2024-2025 eastern elongation and the start of the 2025-2026 western elongation.	5

News and Notes

Phosphine and Ammonia detected in the Atmosphere of Venus

In 2020, Jane Greaves of Cardiff University and her colleagues used the James Clerk Maxwell Telescope to observe Venus in June 2017. They announced that they believed they had discovered phosphine in the atmosphere of Venus [1]. On Earth, Phosphine is a biomarker and there was some suggestion that the Phosphine on Venus may be generated by primitive microbial life in the clouds of the planet. We reported on these results in the Journal [2] and it is fair to say that there was some scepticism towards the results.

Recently, Dave Clements on Imperial College London who is part of the team working with Greaves, believes that the original technical objections to the teams results have now been resolved and furthermore, the preliminary results of recent observations made using a new instrument on the James Clerk Maxwell telescope continued to point to the existence of Phosphine in the atmosphere of Venus. In addition to this, it seems that ammonia has now also been detected.

The detection of ammonia using the Green Bank radio telescope is an additional puzzle and like phosphine, it can be a biomarker. The presence of ammonia in the atmosphere of Venus is as difficult to explain as the phosphine, but some scientists now believe that ammonia could help microbial life to survive the harsh acidic clouds of Venus. Of course, phosphine is generated by active volcanos – and we now have tentative evidence of active volcanism on Venus (observations of which are being pursued by our own Section Members!) so perhaps this is part of the answer.

The ESA Jupiter Icy Moon Explorer (JUICE) will be flying past Venus in August 2025 and observations of Venus could be made by JUICE if the flight engineers were to agree to it- it would be rather ironic if JUICE was to provide the first evidence of life beyond Earth in the harsh clouds of Venus rather than the icy moons of Jupiter!

[1] Greaves J.S. et al., 'Phosphine gas in the cloud decks of Venus', *Nat. Astron.* (2020)

[2] Abel Paul G., 'Life in the Venusian Clouds', *J. Brit. Astron. Assoc.*, **130**, 5, 2020

Observing Mercury's tail during March 2024

Chris Hooker, Mercury co-ordinator

Introduction

In issue No. 10 of Messenger (June 2022) I described the equipment and techniques I developed for imaging Mercury's sodium tail and presented some images of this interesting and little-known phenomenon. Since then there have been a few more opportunities for imaging the tail, first in April 2023 (reported in Messenger issue No 12) and most recently during the eastern elongation in March this year. This article describes the improvements made to the imaging setup since last April and presents the observations made during March, with some analysis of the images obtained.

The occasions when Mercury's tail can be observed are infrequent and relatively short because several factors must combine favourably. First, Mercury must be within about 10 days of elongation. Second, it must be visible at an altitude of 3 degrees or more in a dark or twilight sky with the Sun at least 10 degrees below the horizon: this restricts the observations to periods when the ecliptic is at a sufficiently steep angle to the horizon. Third, Mercury must be in a part of its relatively eccentric orbit where it is approaching or (preferably) receding from the Sun. At such times Mercury's radial velocity is large enough that the sodium absorption lines in the solar spectrum are Doppler-shifted away from the wavelengths where the sodium atoms in the tail absorb light. Finally, and by no means least, the sky must be clear and transparent down to the horizon in the relevant direction!

The period in spring 2024 when the first three conditions were satisfied ran from the 22nd to the 31st of March, with a day or two at either end when I felt it would be worth trying to observe something if conditions were good. In practice there were five days when the weather was good enough, and I was able to capture images of the tail on four of them: the 23rd, 24th, 29th and 30th.

Equipment upgrades

In June 2023 the BAA Council awarded me a Ridley grant towards the purchase of a high-quality narrowband sodium filter from the US company Alluxa. The filter arrived in July, and on testing it I found it had the expected 2.1 nm bandwidth, more than 90% transmission at the sodium wavelengths and had no significant internal reflections. The filter I used previously, by comparison, had 3.5 nm bandwidth, 55% maximum transmission and a wedge that gave rise to multiple internal reflections. These had to be dealt with by carefully orientating the filter to position the duplicate images away from the region of interest. The new filter is better in every important respect!

Since April 2023 I have made several upgrades to the setup, with the goal of improving both the image quality and the guiding. I replaced the two achromatic doublet lenses in the re-imaging optics with proper camera lenses: a 55mm F/2 Super Takumar from an old Pentax SLR (not DSLR!) camera and a 25mm F/1.4 Navitar CCTV lens bought from Thorlabs. Both lenses were designed to give flat fields over an area at least as large as the sensor of the imaging camera. They were mounted facing one another with the CCTV lens nearest the camera, and the new filter in a custom-made holder between them. The mounting hardware is an assembly of lens tubes and thread adapters also bought from Thorlabs. The lens combination acts as a 0.45x focal reducer which relays

the primary image from the telescope onto the sensor and reduces the focal ratio from F/5.9 to F/2.7. Finally, I replaced the ZWO ASI174 camera used previously with a ZWO ASI178MM, which has 2.4-micron pixels and thus samples the image more finely. Figures 1 & 2 below show an image and a schematic of the improved setup. A thin strip of Baader photographic solar filter with the aluminium coating chemically removed from one side is mounted in the telescope focal plane. This filter has an attenuation factor of about 70x in the visible.

Figure 1. Photo of the new re-imager. Description in text.

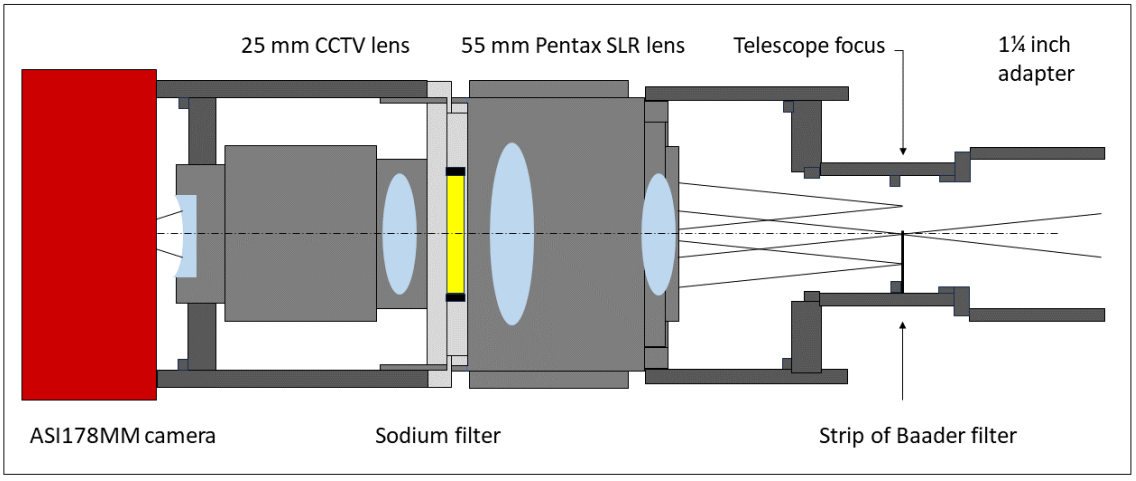

Figure 2. Schematic of the new re-imager showing component layout.

Manual guiding during the 30- to 60-second exposures needed for the tail was tedious and not always satisfactory, and I decided to use autoguiding to keep the image stable. Autoguiding on a star or, in this case, Mercury itself, is a technique normally used for deep-sky imaging. For a planetary imager it represented what my former group leader called “a significant learning opportunity”, or in layman’s terms a chance to bang my head against several different brick walls at the same time. I was eventually able to make the guiding work using ASCOM and PHD2 with a home-

made guiding system built from an old ZWO ASI120MM camera and a 75 mm focal length achromatic lens. This system was used to control my HEQ5-Pro mount via its ST-4 port. The guiding accuracy was typically ±2 arc seconds, which was perfectly acceptable given the image scale of about 2.7 arc seconds per pixel and the expected extent of the tail of up to a degree in length.

The telescope used for these observations is a William Optics ZS66 semi-apo refractor with a focal ratio of F/5.9, which is reduced to F/2.7 by the re-imaging optics. The telescope and re-imager were mounted on a piece of MDF sheet, with a Vixen dovetail rail attached to the underside to allow it to be mounted on the HEQ5-Pro mount. Also on the MDF base-plate were the guide camera, held in an adjustable mount so it could be aimed at the guiding target, and a red-dot finder for initial alignment. Figures 3 & 4 show an earlier version before the change to the SLR lens, but the setup is otherwise identical. To focus the image, the main camera display was zoomed in on a star. The holding ring around the tube near the camera was unclamped so the tube could move within it, and the telescope fine-focus control adjusted while observing the image. Once the best focus was found the holding ring was clamped again to keep the camera position fixed for the duration of the session.

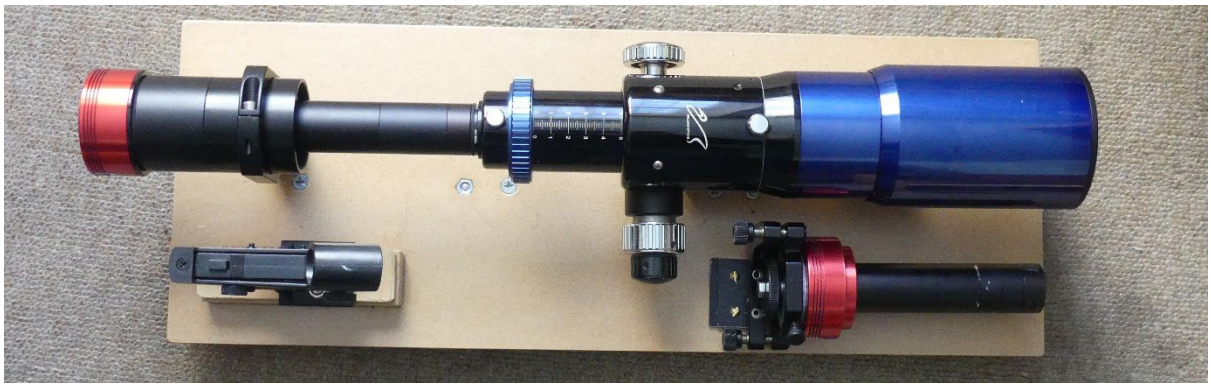

Figure 3. Complete setup for imaging Mercury's tail, including finder and guide camera.

The setup is designed to be portable, so it can be used at a remote site with a clear eastern or western horizon. There are a few good locations less than 20 minutes' drive from where I live that are easy to access and are relatively private.

For evening observations, polar alignment can be an issue, as the tripod has to be set up before each observing run. I have developed various methods for doing this, including a levelling device that fits into the dovetail and allows the altitude of the polar axis to be set. Once the sky is dark enough, Polaris can be found by rotating the mount in azimuth while looking through the polar finder. I

usually mark the final positions of the tripod legs by some means such as chalk marks or scratches on the ground, so that setting up on subsequent occasions is quicker.

Figure 4. Imaging setup on the HEQ5-Pro mount.

Observations during March 2024

Mercury's radial velocity on 23rd March was 5.6 km s^{-1}, similar to when I recorded an extended tail in April 2023. Mercury was quite bright at magnitude -0.4, so the attenuating strip was necessary to avoid it becoming severely overexposed due to the long exposures needed for the tail. On the 24th I made some changes to the filter strip so it was better-placed in the field; however, the session was cut short by clouds moving in. There followed four days of thick cloud, strong winds and heavy rain, but on the 29th the weather improved. I was able to capture some more images, despite problems with the guiding software which meant I had to rely just on the polar alignment and the mount to track Mercury. On the 30th I resolved the guiding issues and captured the best images of the session, with the tail extending for over 1.6 million kilometres. A selection of images from this period is shown here.

Figure 5. Mercury's tail on 23rd March, 19:30 UT. Length of tail 1.3 million km.

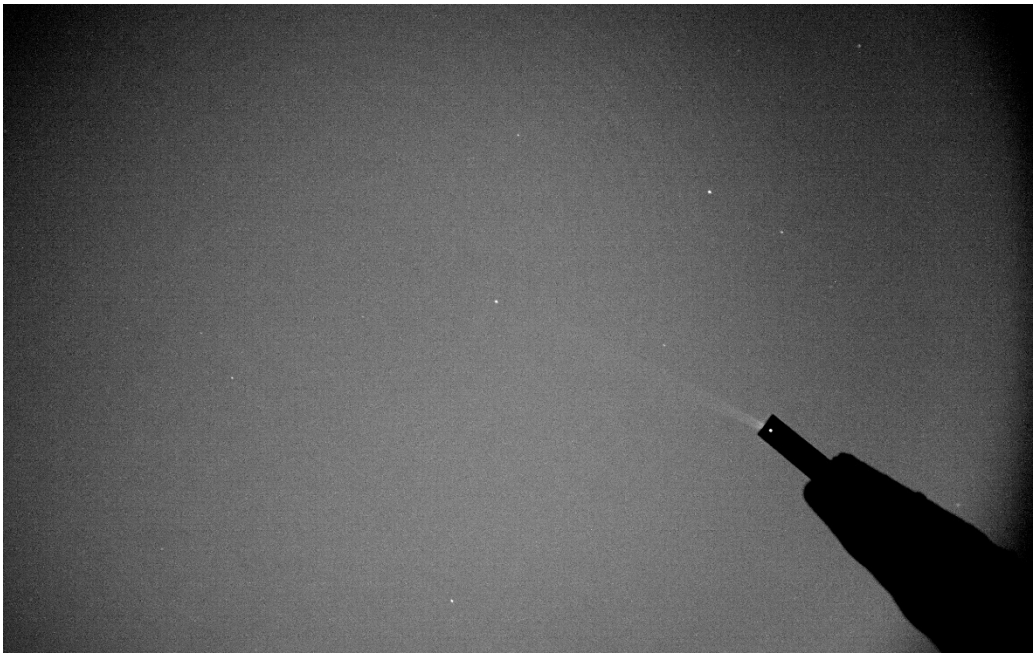

Figure 6. Mercury's tail on 24th March, 19:26 UT. Length of tail 1.4 million km.

The final image is from the 30th March, when Mercury's radial velocity was 9.5 km s^{-1}, almost the maximum possible. Mercury had passed eastern elongation and was now a crescent, moving back towards the Sun and visibly fainter at mag 0.93. The time available for imaging was short, so rather than delay by positioning Mercury behind the filter strip, I simply positioned it near the end of the strip and started guiding. The tail was strongly excited and had a detectable extent of 1.67 million km.

Figure 7. Mercury's tail at 19:44 UT on 30th March, the best image from the recent elongation.

There are a couple of points to note about the appearance of the tail, especially in the final image (Figure 7). The tail is expanding as it moves away from Mercury, but its shape is not a narrow triangle with Mercury at the apex: in fact, the outline of the tail is a parabola. The reason is that the sodium atoms leaving Mercury have a constant velocity perpendicular to the Sun-Mercury line, determined by the speed that was imparted to the atoms as they were sputtered out of the surface, later reduced by the gravitational pull of the planet. In the direction along the tail, on the other hand, the atoms are continually accelerated by the absorption of photons from the Sun, which increases their momentum in the anti-solar direction. When an atom returns to the ground state the resulting photon is emitted in a random direction, which over repeated cycles of absorption and re-emission does not change the average transverse velocity of the atom.

A calculation of the acceleration of sodium atoms irradiated by sunlight in the vicinity of Mercury was found in a paper dealing with the tail, and the value is 3.3 m s^{-2}. From this acceleration and the measured extent of the tail, the time required for atoms to travel the length of the tail was calculated to be around eight hours. The velocity of atoms down the tail can exceed 100 km s^{-1} compared to the transverse velocities of a few km s^{-1}, which accounts for the greatly elongated shape of the tail.

The second point to note is that the upper (northern) side of the tail is more sharply defined in the region further from Mercury, whereas the other side becomes indistinct about halfway to the end of the visible part. This reflects the uneven distribution of the sodium sources on Mercury's surface plus different sputtering rates that result from the interactions of the solar wind with Mercury's magnetosphere. The formation of the tail is a complex process which is not fully understood even now.

The parabolic shape of the envelope of the tail was verified by measuring the width of the tail at seven distances from Mercury on the image from the 30th March. A graph of the width against the square root of the distance is a straight line (Figure 8), as would be expected for a parabola.

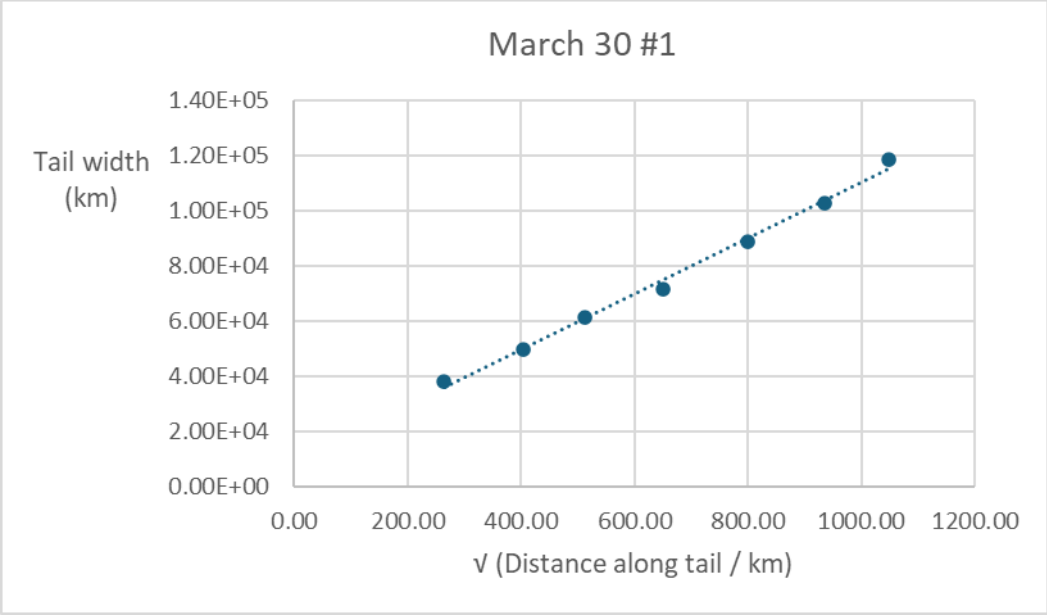

Figure 8. Graph of the width of the tail vs √ (distance from Mercury).

On this occasion there were no visible disturbances in the tail due to interactions with, for example, coronal mass ejections. Capturing such an event would be very lucky, given that sodium atoms travel down the visible length of the tail in only eight hours. The time window for a CME to hit Mercury and produce an effect on the tail that was visible in a terrestrial image would be about the same as the transit time, adding a further low-probability factor to the set of conditions to be met. The next opportunity to observe the tail occurs during the western elongation in December 2024. The Sun will still be fairly active at that time so there may be a chance of capturing the effect of a CME on the tail.

Venus Night-side Imaging - Measuring the Signal to Noise Ratio (SNR)

Martin Lewis

Overview

By imaging the night-side of Venus when close to inferior conjunction, and by using a narrowband filter, centred around 1010nm, one can see through the planet's normally opaque sulphuric acid clouds and capture details on the planet's hot surface. Such details are seen to correlate with topographical features on the surface. The method also has the potential to detect signs of possible volcanic activity on Venus.

Imaging features on the Venusian surface is a difficult challenge and low-noise/high-resolution images are particularly hard to achieve. The night-side signal is faint and to prevent it being swamped by twilight, imaging needs to take place when the Sun is just below the horizon, meaning the planet's altitude is low. Additional difficulties arise because the night-side region is sited immediately adjacent to the much, much brighter dayside crescent.

Signal to noise ratio (SNR) and resolution are the two key indicators of night-side image quality and these dictate the levels of surface detail that can be seen. By taking a line-profile through stacked, unstretched images of the night-side, and by measuring the grey-level brightness along that line, it is possible to understand the impact of camera settings, geometry and sky brightness on the measured SNR values. Doing so gives insights into what conditions of camera and sky are best for amateurs wanting to image night-side surface details.

Main Findings

- To minimise noise due to twilight, image when the Sun is 6° or more below the horizon
- Image when the phase of dayside crescent is small and the planet large to minimise glare, which reduces the SNR of the night-side
- Don't worry about read noise when imaging with modern planetary cameras
- Use 12-bit imaging as standard
- It is worth trying exposures of 25msec (at f4.5 and 12-bit mode) or less to reduce atmospheric smearing effects to help improve resolution

Introduction

This article details the analysis of images gathered during Venus night-side imaging sessions during September 2023 - a morning apparition which was particularly favourable for Northern hemisphere observers (figure 1). Data was gathered with a 444mm Dobsonian scope, operating at native f4.5. Videos were taken with a Player One Uranus-C camera with the protection glass removed to reduce scattering from the dayside crescent (the camera sensor cover glass was not removed). In front of the camera was placed a PixelTeq 1010nm filter with a 38nm bandwidth. The

PixelTeq filter was placed in series with a ZWO 850nm filter, which suppressed residual optical light leakage through the PixelTeq filter.

For more information on the imaging set-up used, and much more on the challenges of imaging the night-side of Venus, see my article in the BAA Mercury and Venus newsletter, Messenger, from March 2024 (#14).

The main intention of this analysis was to understand the principles underlying the imaging of this unusual planetary target, in particular, the reasons underlying choices of gain, bit depth, and frame exposure length.

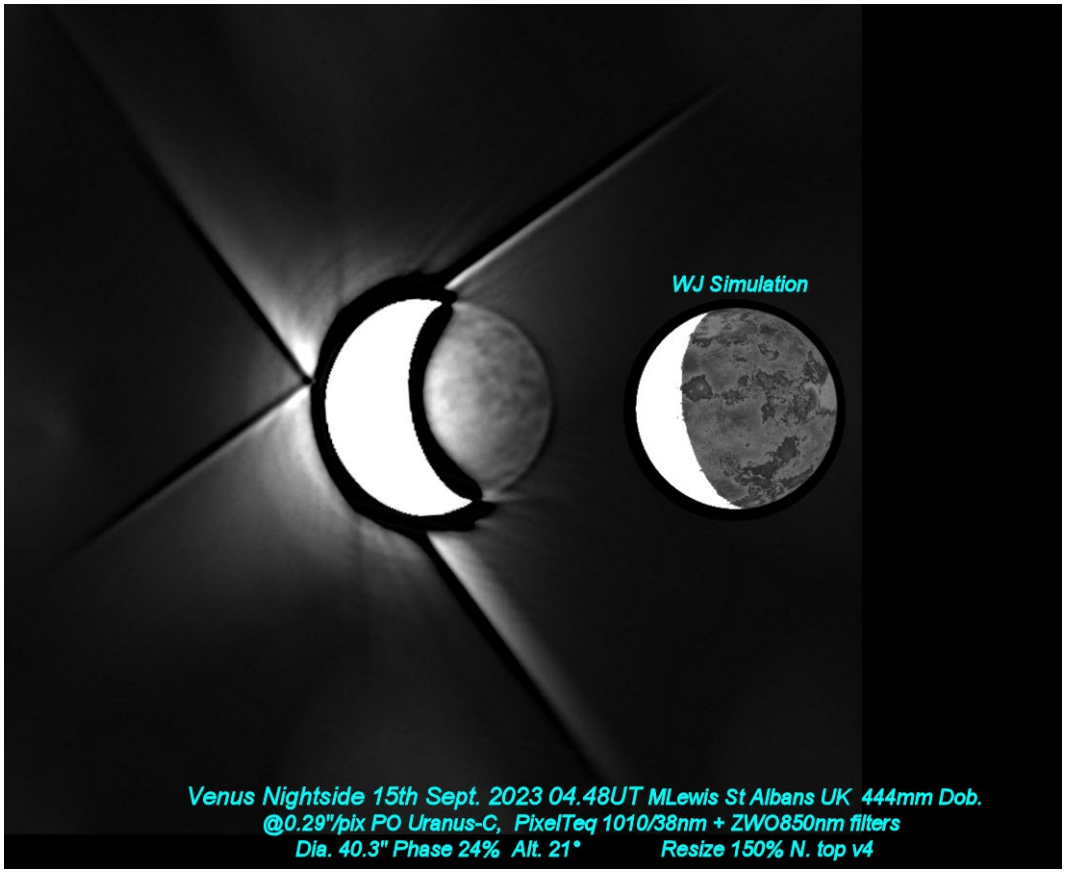

Figure 1. Venus night-side image from 15th September - the author's best morning session and in the middle of the optimum imaging period for Northern hemisphere observers

Quality of Night-side Images

The quality of Venus nightside images for any imaging session is related to the resolution of nightside surface features and to the signal to noise ratio (SNR) of the images. The best night-side images are both high resolution and low noise (high SNR).

For a given telescope set-up/camera and camera settings, the resolution and levels of noise in night-side images are primarily dictated by the following external factors:

- How good the seeing was for the planet that day - affected by atmospheric stability and Venus's altitude. **Affects resolution**
- The brightness of the background sky during imaging. **Affects SNR**
- The prevailing apparition geometry for that session- particularly the size of the crescent and planet's angular diameter. These characteristics affect glare from the dayside, percentage of night-side on show, and angular size of the night-side. **Affects both resolution and SNR**

This analysis looks primarily at aspects of the camera settings, set-up and geometry which affect SNR, rather than exploring aspects affecting resolution. This was done through calculating the SNR at

a chosen reference location in the middle of the night-side, for images captured in different conditions and with different camera settings.

For this study I used three pre-sunrise imaging sessions from September 2023:

- 5-9-2023. Good conditions of transparency and fair seeing, early-on in the optimum imaging period. Experiments carried out on the impact of increasing brightness of the dawn sky
- 15-9-2023. Very good conditions of transparency and seeing, in a darker sky, in the middle of the optimum imaging period
- 23-9-2023. Fair condition towards end of the optimum imaging period. Experiments carried out with different camera gains and exposures

Signal to Noise Ratio Measurement

The SNR of the night-side portion of candidate Venus images can be determined by measuring the value of the isolated night-side signal and dividing this by the magnitude of the noise in that signal.

Noise and signal are not read directly from the images but have to be determined indirectly as outlined below:

<u>Signal</u>

- The isolated night-side signal is the brightness in the night-side region after subtracting off the following sources that otherwise boost the brightness at the reference location:
    - The glare[1] from the dayside portion at that location on the night-side
    - The wash of light across the field from the twilight sky
    - The camera brightness setting (this setting adds a uniform brightness value to all image pixels)

<u>Noise</u>

- The noise in the signal from the night-side region is a function of the following two components which, because they are both essentially random in nature, add in quadrature[2].
    - The Shot Noise of the total signal at the reference location within the night-side region. This is the sum of the light from the twilight sky, the glare and the true night-side component (these value just sum normally - not in quadrature)
    - The Read Noise of the sensor at the chosen gain setting

Brightness Measurement Method

[1] This includes all mechanisms that scatter light from the much brighter dayside crescent into the immediately surrounding region. This includes scattering in the atmosphere, scatter from the telescope optics, scatter from any filters, scatter in the camera sensor itself, and in my case, diffraction from the secondary spider vanes of my Newtonian reflecting telescope

[2] Quadrature means the result is the square root of the sum of the square of the individual components i.e. $s = \sqrt{a^2 + b^2 + c^2}$

The signal and noise values at the reference location for each of the chosen videos were based on careful measurement of the stacked but unstretched final images. These stacks were generated from standard processing of each video in AutoStakkert!4. Brightness measurements used to calculate noise and signal, were made using the readily available and widely-used freeware program, Image J.

The Image-J measurements involved taking a line-profile across each of the stacked images of Venus. Each line was drawn so that it started in the centre of the over-exposed dayside crescent, ran across the middle of the night-side portion, and ended approximately one Venus-diameter away, in the darker background region. A check was made that this end-point was well away from any secondary reflection of the dayside (an issue that afflicts CMOS sensors operating at these wavelengths). The profile line length was chosen so its mid-point was located right on the dark limb of the planet.

To achieve some consistency in the analysis from session to session, measurements of the night-side brightness, from which signal and noise were determined, were all taken at the same reference position on the profile line, 31% of Venus's diameter inbound from the limb. Although a slightly arbitrary reference position, this was exactly 50 pixels in from the limb for the images on 5th September (figure 2) and was in the centre of the night-side region in images taken on 15th September - the middle of the optimum imaging period (see figure 3).

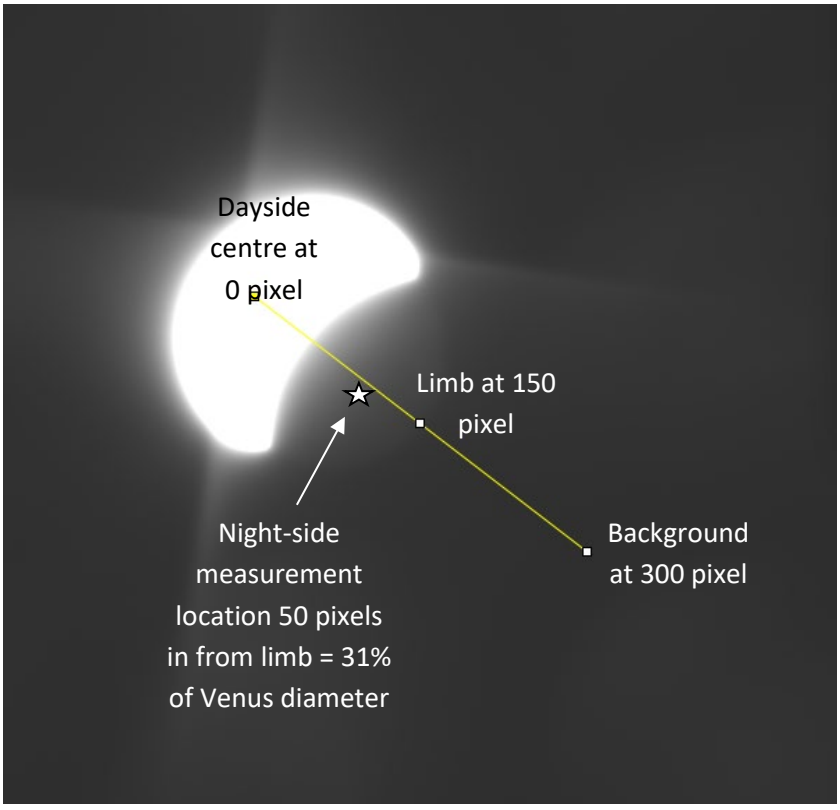

Figure 2: Measurement line drawn in Image J for earliest image on 5th September. Note: Image is brightened in the figure to reveal the night-side, however, the actual brightness measurements were taken on the unbrightened stacked image.

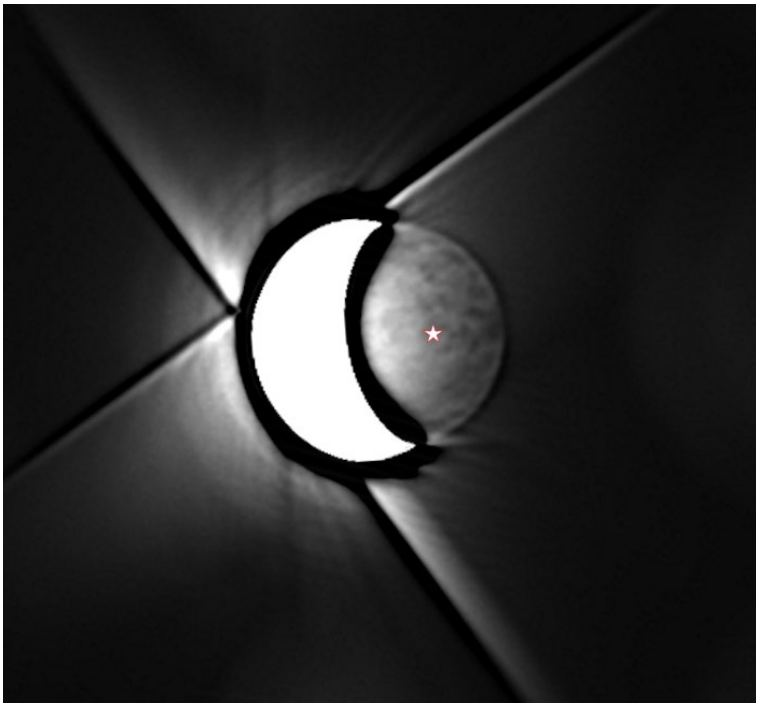

Figure 3: Reference night-side signal and noise measurement location 31% in from limb, marked on the image of the 15th September - around the middle of the optimum imaging period. The reference location sits right in the middle of the night-side region for this date.

For each session, account was taken of the decreasing size of the planet through September. The distance in pixels from the limb was therefore altered in proportion to the angular diameter of the planet, to maintain the reference position at 31% of the planet's diameter in from the limb, as below:

- 5th September. Planet diameter 47.0". Reference location 50 pixels in from limb
- 15th September. Planet diameter 40.3". Reference location 43 pixels in from limb
- 23rd September. Planet diameter 35.7". Reference location 38 pixels in from limb

The brightness at each pixel position along the measurement line was tabulated by Image-J and imported into Excel. This data was then used to plot brightness values with pixel position. An example plot is shown in figure 4a below; this is from the earliest video at 04:42UT on 5th September, with the Sun 5.6° below the horizon.

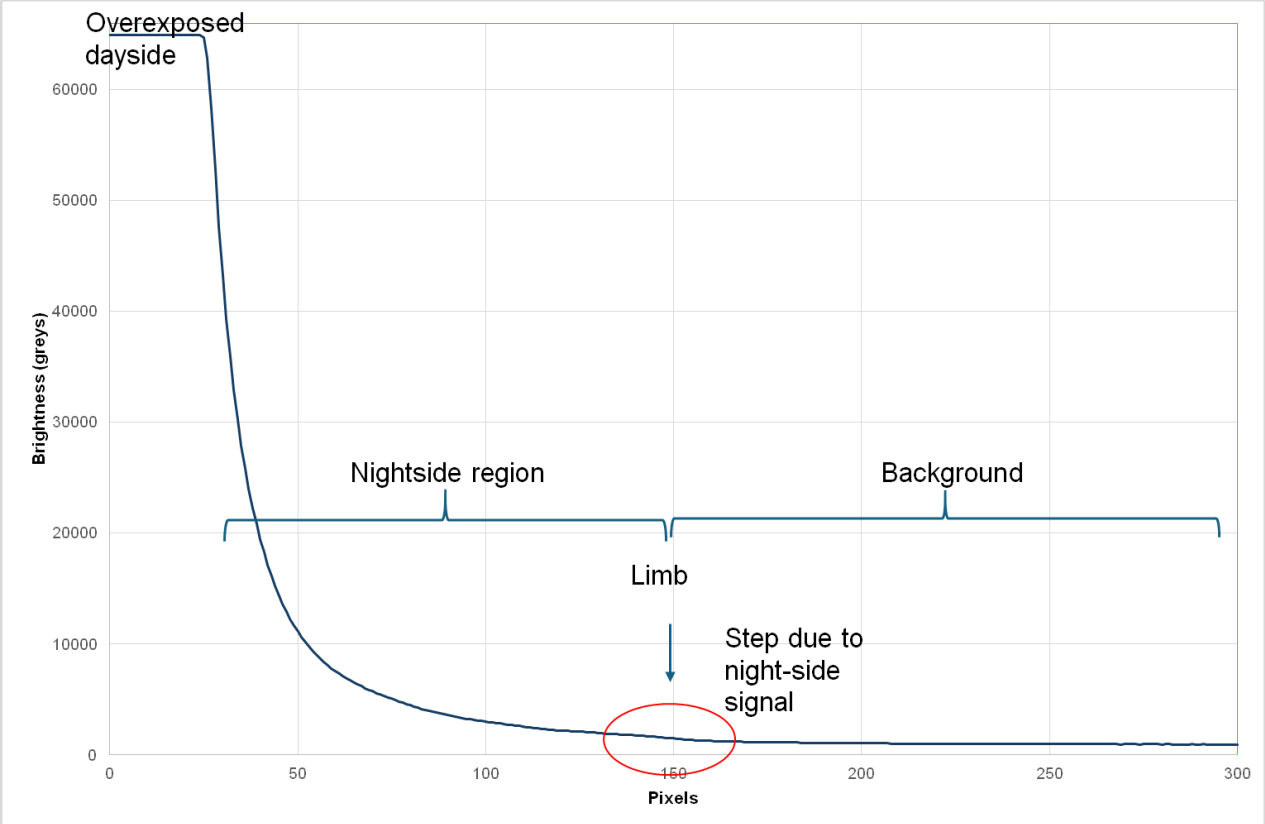

Figure 4a: Change in brightness with pixel position along the line shown in Figure 2, for the earliest Venus video taken on 5/9/2023

Working left to right in figure 4a: The brightness of the background is low and fairly level on the right hand side, as the sky was fairly dark at the time of capture. As you approach the limb, however, you will see that the brightness value jumps up fractionally as you move from the background onto the limb of the planet, at about the 150 pixel position. This step-change is actually our precious night-side signal that we wish to measure! The brightness rises sharply as you move further left on the plot towards the dayside - the glare increasing dramatically as you approach the bright crescent. As the dayside is some 20x overexposed, it is saturated, creating the flat portion of the plot on the extreme left.

Figure 4a nicely demonstrates the difficulties of night-side imaging - the true base IR night-side signal really is pretty small compared to the brightness of the background and is also much smaller than the dayside glare, particularly as you approach the dayside crescent. What is more, we don't want to just be able to detect this step, we want to be able to see real variations in this small increase in brightness; the variations in this step with position are the signal of the surface features we wish to capture.

You get a better feel for this night-side step in brightness in figure 4b, below, where the vertical axis is expanded by ~6.5x.

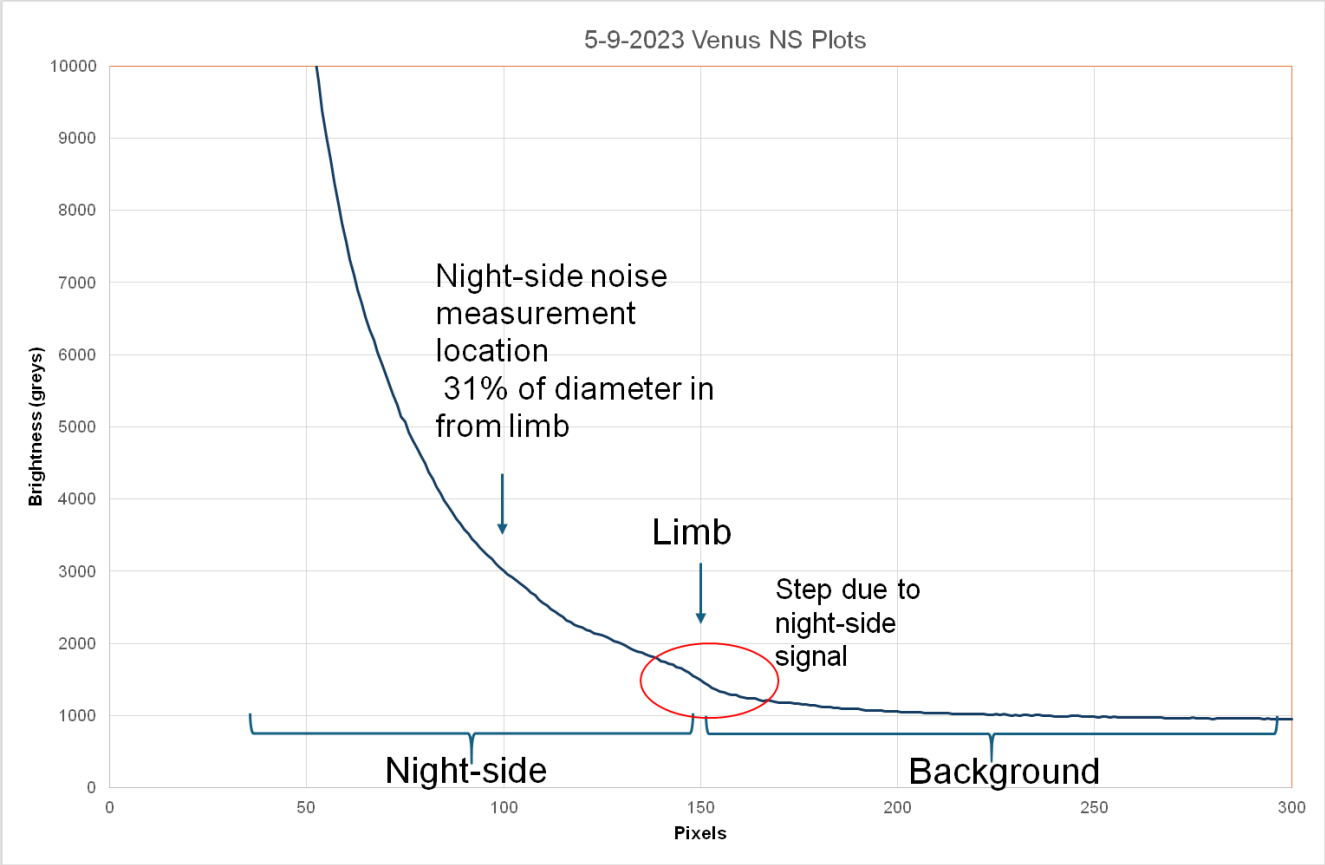

Figure 4b: As figure 4a but with vertical axis expanded to better show step at limb

The key parameter to measure from figure 4b is the size night-side signal - the brightness step at the limb. One way of making an estimate of this step size is by subtracting off trial values from all the pixels along the measurement line *just* in the night-side portion. Different trial values are tried until the subtracted night-side curve seems to connect smoothly with the curve that continues on into the background sky. Hopefully, figure 4c will make this clearer, which uses a trial subtraction value of 200. This trial value seems to be about right, with a smooth extrapolation to meet the curve of the background. It means that the night-side brightness for the 5th September image is estimated at just 200 grey levels, compared to the saturated level of ~65,000 for the dayside (maximum value for 16-bit stacked image).

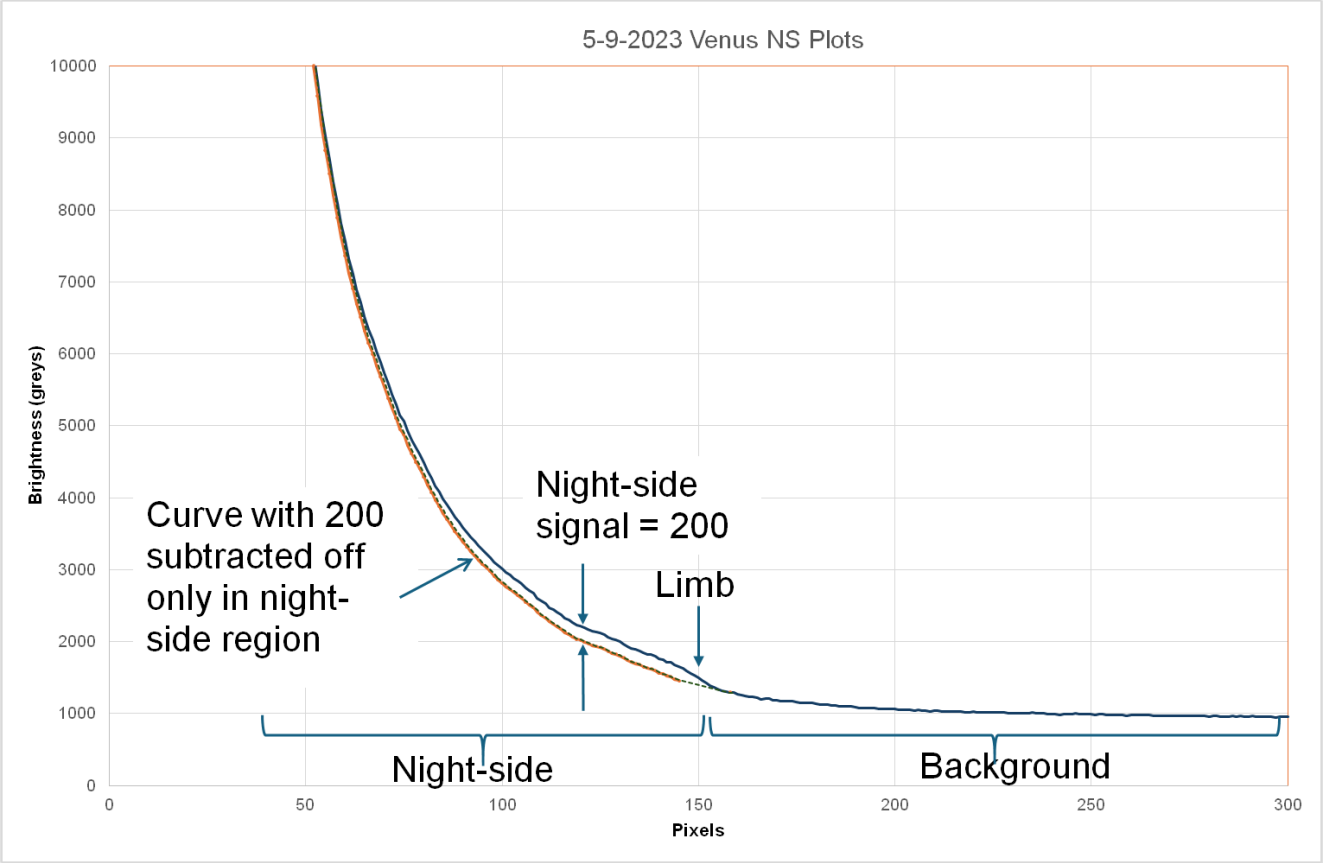

Figure 4c: As Figure 4b but with trial value of 200 subtracted off night-side region so it smoothly blends with curve for background sky. In this case night-side brightness is thus estimated as 200.

In figure 4b, you can see that the brightness at our 31% of diameter reference location (at the 100 pixel mark for that plot) is about 3,000, with the background brightness leveling out at about 1,000. This means that at our reference location the background[3] accounts for 33% of the total signal, the glare makes up 60%, whilst our night-side base signal of 200 makes up just 7% of the total signal[4]. For data gathered during the imaging session that morning, as you will see, twilight starts to increasingly dominate the brightness signal once the sun is higher than the -5.6° altitude it was for the data in figures 4a and 4b.

The night-side trial value subtraction technique, described above, was used on all the selected images from the three sessions to give a measured estimate for the base night-side brightness in each of the stacked images, at the same 31% of diameter reference location.

[3] Note that part of the signal from the background may be glare or light diffracted from the secondary vanes rather than purely twilight.

[4] To keep things simple, the uniform camera brightness setting mentioned previously has already been taken off the signal values in all these plots and calculations

It should be noted that the estimated base night-side brightness values we have measured in the stacks will be the same as that in the individual frames making up the videos. This is because stacking does not increase the image brightness. The frames however will be 12-bit images[5] with only 4,096 grey levels compared to stacked images which are 16-bit with ~65,000 grey levels. This makes the value of the grey level brightness for the night-side in the frames some 16x lower. This means that in our example where the night-side brightness in the 16-bit stack was 200 grey levels, in the frames it will be 200/16 or just 12.5 grey levels.

Noise Determination

Now we have a method of determining the base night-side signal for our Venus images, attention has to turn to the determination of the magnitude of the noise in that signal at our 31% reference location. Once we have done this, the noise value can then be just divided into the signal value to determine the SNR for each image.

To calculate the noise for the stacked images first we need to determine the level of noise in individual *frames*, then go from there. Once the frame noise is known, you can work out the improvement you get from stacking multiple frames with that level of noise in each frame to work out what the noise will be in the stacked image.

Noise in Frames

The frame noise at the 31% position can be calculated by adding the frame read noise and the shot noise at that location. Shot noise is random in nature and generally read noise is too, in which case the two add in quadrature as described before:

$$\text{total noise} = \sqrt{([\text{short noise}]^2 + [\text{read noise}]^2)}$$

It is well-established that the variation in the number of electrons making up the CMOS sensor signal, the Shot Noise (also known as quantum noise), is equal to the square root of the number of electrons in that signal. We can use this fact to get a measurement of the magnitude of the noise from knowing the size of the signal, however, it all has to be worked out in numbers of electron, then later converted back to grey-levels.

- Shot noise. The shot noise can be calculated for the 31% location by determining the brightness here and working out find the corresponding shot noise in electrons. This is done in the following way:
    - Find the grey-level brightness at the 31% position on the stacked image – this will be the sum of the glare, the background, and the base night-side signal at that site. Note: As stated previously, the brightness at any position in the stacked image should be same as the brightness in individual frames, so it is valid to use the stacked image to find the local brightness of frames. The stacked image is much less noisy than the frames, and this makes it much easier to determine an accurate local brightness.
    - Use the camera manufacturer's data to work out the number of electrons that this brightness equates to at the chosen gain.

[5] Assuming camera the 16-bit mode was ticked otherwise frames are only 8-bit - more about this later

        - For example, in figure 4b for the 31% position on the stacked image, the local brightness is 3,000. A camera gain of 300 (30dB) was used for that video and for gain=300 the manufacturer's data says the camera needs 0.022 electrons per (16-bit) grey level. Therefore a brightness of 3,000 equates to a pixel signal per frame of 66 electrons (3000x0.022=66)
    - The shot noise is then simply given as the square root of the number of electrons measured above. In our example shot noise is √66 or **8.11e$^-$**
- Read noise. This value is quite easy to find and can be obtained from camera supplier data who will quote values of frame read noise in electrons for given camera gain settings. In the example above with a gain of 300 the read noise is given by Player One as **0.9e$^-$** .

Frame SNR

- For our example we can now combine the read noise with the shot noise using the quadrature equation. This gives noise=√(8.112 + 0.92) giving **8.16e$^-$** as the total noise at the 31% location for the individual frames.
- We now need to convert this value to grey levels. Frames are 12-bit rather than 16-bit, with a maximum of 4096 grey levels, and we can convert the noise value we found to 12-bit grey levels by first dividing by the 16-bit gain related conversion factor (0.022e$^-$ per grey level) and then dividing the answer by 16x (to convert from 16-bit to 12-bit). If we do that we get 8.16/(16x0.022)=23.3 grey levels as the calculated noise value for the reference location in the frame.
- Finally, we can calculate the SNR for the 12-bit frame. This is done by dividing the base night-side signal we found previously, by the magnitude of the noise. As we found the signal to be 12.5 grey levels (12-bit) and the noise to be 23.3 (also 12-bit) , the SNR for the location in the frame comes out as a very low **0.536.**

Noise in Stacked images

Much more important than the SNR of frames is the SNR of stacked images, because it is the stacked image which goes to form the final master image, possibly by combining it with other stacked images to further improve SNR.

In stacking, the magnitude of the signal does not change but the noise is reduced by the averaging effect of stacking random data in the frames that make up the stack. If we want to go from the SNR of frames to the SNR of stacked image, we use the rule that the noise reduces by √N where N is the number of frames stacked. If there are 400 frames, the noise would be reduced by 20x if 40,000 frames it would be reduced by 200x.

In our example video, I stacked 90% of 1595 frames, so this reduces the noise by √(0.9x1595)=37.9x. Thus the SNR of the reference location in the stacked image is 37.9x better than that in the individual frames that go to make up the stack. This gives 37.9x 0.536 = **20.4** as the calculated SNR for the reference area in our example stacked image.

SNR Results

Using the methods described above, I was able to compile an Excel spreadsheet giving camera settings, manufacturing data, image measurements and various derived values of noise and SNR. A summary table showing the key information is shown below. The much larger spreadsheet with all the data is available from the author on request (martin@skyinspector.co.uk).

Date	Time	Solar Altitude	Camera Exposure Gain	Frames in video Note 1	Bgnd + NS + Glare signal in GLs of 65356 Note 2	Background as % of total brightness at ref location	Glare as % of total brightness at Ref location	NS signal in GLs of 65355 (stack)	NS signal as % of Brightness at Ref location	NS signal in GLs of 4096 (frame)	Frame total noise in greys of 4096	Read noise contribution as % of total noise in stack	Frame SNR	Stack SNR
05/09/2023	04:42	-5.6°	75msec G300	1595	3009	32%	61%	200	6.6%	13	23	1%	0.5	20.3
05/09/2023	04:46	-5.0°	75msec G300	1581	4037	47%	48%	200	5.0%	13	27	1%	0.5	17.5
05/09/2023	04:52	-4.2°	100msec G300	1176	10329	72%	25%	270	2.6%	17	43	0%	0.4	12.8
05/09/2023	04:56	-3.6°	100msec G300	1173	23333	87%	12%	270	1.2%	17	65	0%	0.3	8.5
05/09/2023	05:08	-1.8°	100msec G240	1183	34264	95%	4%	135	0.4%	8	55	0%	0.2	5.0
15/09/2023	04:46	-7.6°	75msec G260	1558	2493	11%	85%	85	3.4%	5	15	1%	0.4	13.3
23/09/2023	04:35	-11.3°	25msec G260	4766	1257	10%	88%	29	2.3%	2	12	2%	0.2	9.9
23/09/2023	04:33	-11.6°	75msec G260	1598	3345	7%	91%	84	2.5%	5	19	1%	0.3	10.2
23/09/2023	04:37	-11.0°	225msec G260	518	10205	5%	93%	254	2.5%	16	34	0%	0.5	10.1
23/09/2023	04:43	-10.1°	25msec G370	4714	4004	8%	90%	100	2.5%	6	40	2%	0.2	10.1
23/09/2023	04:46	-9.6°	75msec G275	1557	4052	6%	92%	100	2.5%	6	23	1%	0.3	10.0
23/09/2023	04:40	-10.5°	225msec G180	501	4729	5%	93%	100	2.1%	6	15	4%	0.4	9.0
Note 1	Stacks all 90% of total frames													
Note 2	After substracting off camera brightness setting													

Table 1. Summary analysis table giving calculated stack & frame SNRs

ANALYSIS

Effect of twilight on SNR

The first five rows in table 1 show the huge impact of the brightening sky on the SNR with its value for the stacked image dropping from 20.3, with the Sun at an altitude of -5.6°, to an SNR of just 5.0 some 26mins later when the Sun was only 1.8° below the horizon. In the darker sky, with a solar altitude of -5.6°, the night-side signal was 6.6% of the total signal at the reference location, whilst later on with the Sun at -1.8° the much brighter sky means that the night-side represented just 0.4% of the total signal. It is the much brighter sky and the correspondingly much higher shot noise associated with the higher signal, which causes this big drop of the SNR as we approach sunrise.

In figure 5, below, you can see the rising background brightness with time over the space of just 14 minutes. The data has been normalised so that all the curves are corrected to a camera exposure time of 75msec and Gain 300 (the upper two were actually taken at 100msec exposure plus a gain of 300, which would have exaggerated the effect of the brightening sky).

Figure 5: Line profile for images taken over a 14min. period on 5/9/2023 showing climbing sky brightness as the Sun approaches sunrise. Background brightness are given for each altitude relative to that at 04:42UT

An interesting question that this analysis prompts is, 'What is the solar altitude at which the sky can be considered essentially *dark* whilst imaging the night-side?'

To answer this, we can take data for the background brightness for different solar altitudes and again correct it to camera settings of 75msec and G300. If we do this and plot that background brightness against altitude, we get the plot in figure 6. This shows that the background brightness really starts to rise at about -6°. Hence we can take -6° as our reasonable 'true dark' limiting altitude.

At -6° the normalised sky brightness is 500 grey levels, so still 2.5x brighter than the base night-side signal. Even at -12° in figure 6 the background is still at about 300 grey levels - 1.5x brighter than the base night-side signal. Some of this residual background signal is twilight sky but almost certainly a proportion is attributable to glare from the very bright dayside and also light diffracted from the dayside by the secondary spider vanes of the imaging telescope. In telescopes without secondary vanes, such as SCTs, I would expect the background brightness to be lower for these solar altitudes.

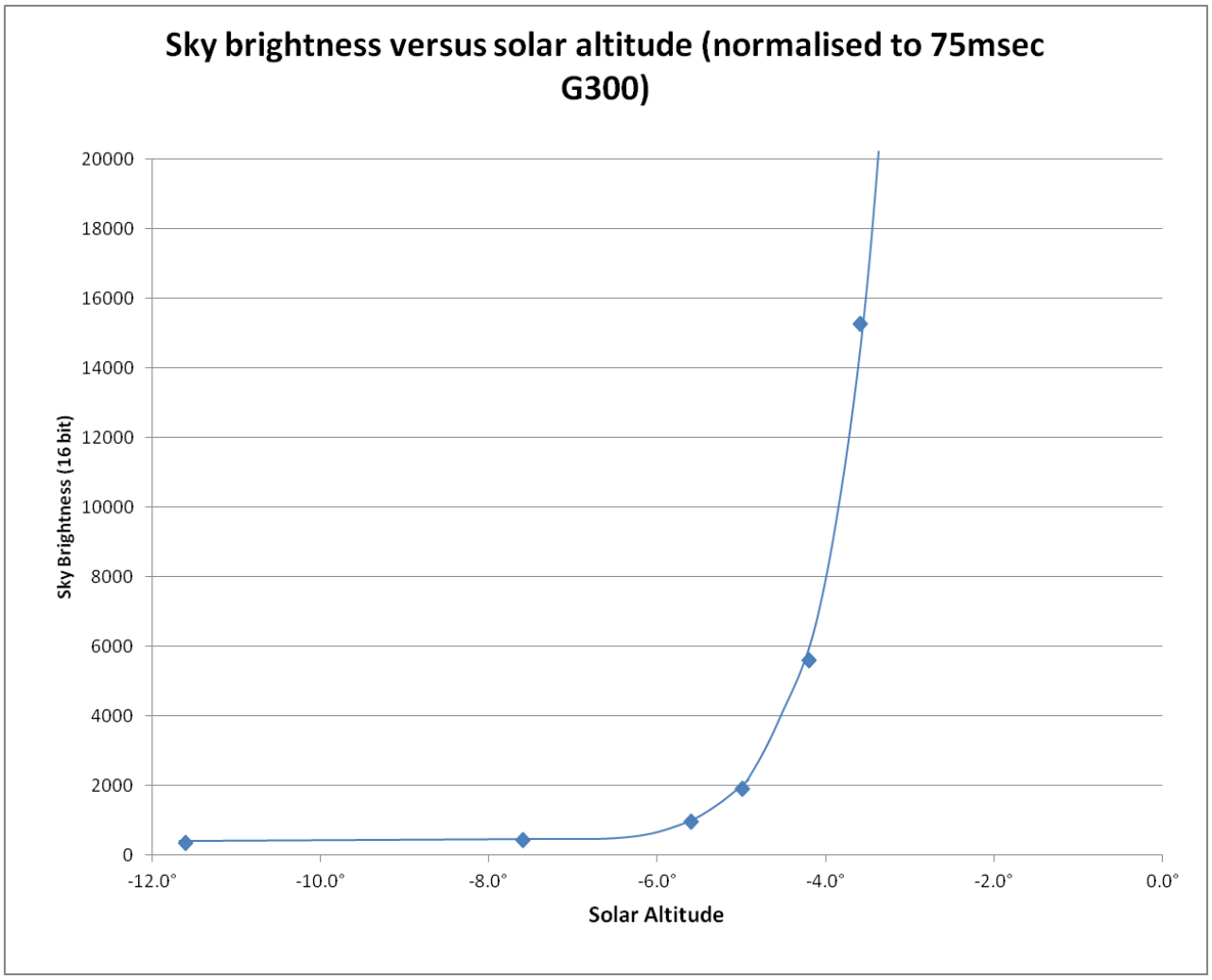

Figure 6: Measured background sky brightness versus solar altitude on 5th Sept. with data adjusted to a common exposure of 75msec & gain 300. See how the sky brightness climbs rapidly at a solar altitude of above -6°. Note the Venus night-side signal is just around 200 on this scale.

To see the impact of the increasing brightness of the background sky on the final processed image from each video I have made the compilation below (figure 7). The compilation shows the solar altitude, the relative sky brightness, the resulting SNR of the stacked (but unprocessed) image, and the processed image itself.

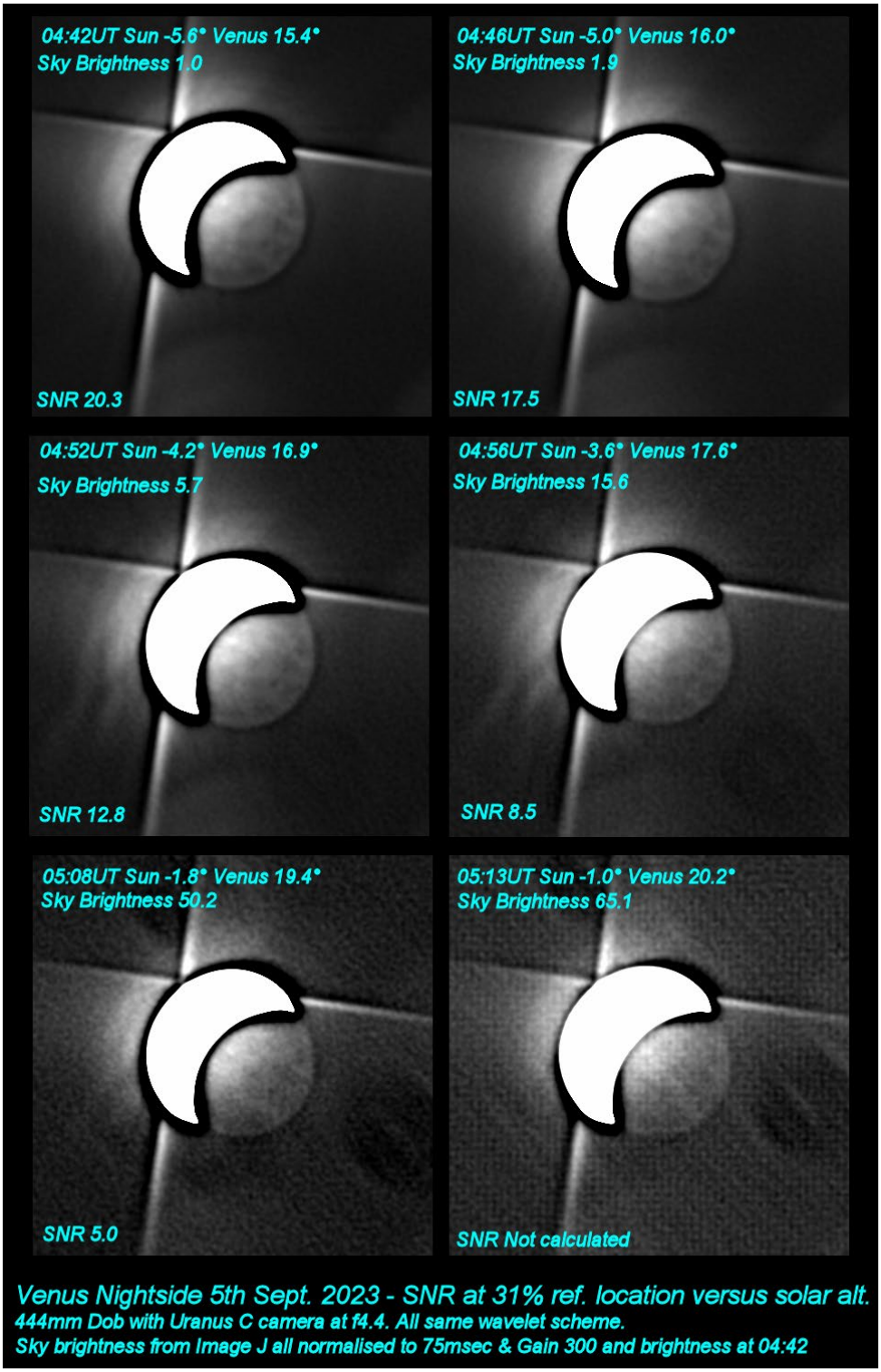

*Figure 7: Processed IR images from 5th Sept. 2023 for different solar and Venus altitudes. The calculated SNRs are given for the **unprocessed**, stacked, images, at the 31% reference locations in middle of the night-side region. Noise gets noticeably worse for a solar altitude of -4.2°and higher. Sky brightness values are given which have been corrected to an exposure of 75msec and gain 300 and the values scaled to the sky brightness at 04:42. At 05:13UT with the sky brightness some 65x brighter than at 04:42, the image takes on a 'woven texture' pattern related to an 8-pixel repeat structure within the IMX585 chip - this is a fairly well-documented phenomenon when operating in the infra-red for this chip.*

Effect of read noise on SNR

The third from last column in Table 1 shows the contribution of the read noise to the total noise at the 31% reference location on the night-side. It shows that with modern low-noise digital video cameras read noise actually plays very little part in the overall noise levels in the final Venus night-side image. Instead, noise is almost completely dominated by the shot (quantum) noise coming from the combined light of the background twilight wash and the glare at that location from the scattered light of the nearby dayside crescent.

At a camera gain of 210 (21dB), the Uranus-C switches to HGC (high conversion gain) mode and the read noise drops dramatically from $3.8e^-$ to $1.1e^-$. The standard recommendation is to always use a gain above the HGC level, because of the higher read noise if operating below this setting. The last line in the table shows data for the camera running at a gain below this recommended minimum of 210. Here the gain was set to 180, leading to a read noise of $4.0e^-$. Despite this higher value, the read noise is still only responsible for just 4% of the total noise in the stacked image.

Balancing Gain and Exposure and the effect of Exposure on SNR

The bottom six rows of table 1 relate to images taken on 23rd Sept at various gains and exposures to determine the impact of these settings on the image quality. Two sets were run:

- Set 1 at fixed gain of 260 with three different exposures having a factor of 3x between each (25msec, 75msec, 225msec)
- Set 2 used the same three exposures but altered the gain setting to maintain the same image brightness - so gain went down by 3x between images as exposure went up by 3x.

Videos from the two sets were processed identically in AutoStakkert!4. In Registax the same wavelet settings were used, however different histogram stretches were carried out - each stretch being appropriate for that image brightness and background brightness. No other processing was used. Results are shown in figure 8 below.

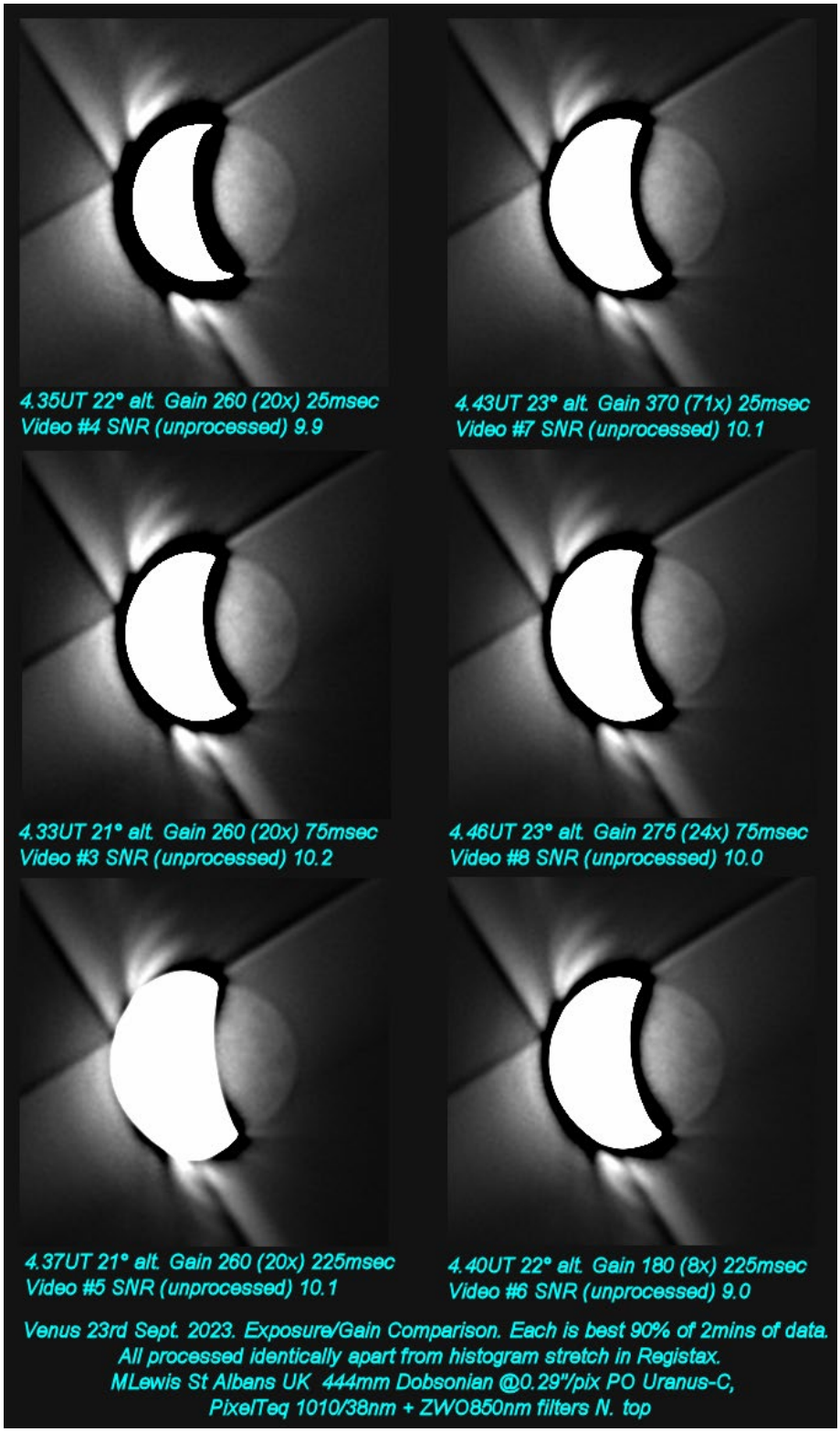

Figure 8: Sets of processed exposure & gain test images taken on 23rd Sept. Top row had constant gain & varying exposure. In bottom row gain & exposure were traded against one another to maintain image brightness. SNRs are given for the stacked but unprocessed images.

Processed images from the trial showed much less of a difference than expected, especially given the large range in exposure and gain. The calculated SNR's are all quite similar, being in the range 9.0-10.2. Comments are:

- The best detail, gauged by the definition in the dark central Aphrodite region, seems to be shown for the 25msec images. This is likely to be as the result of the shorter exposure leading to reduced atmospheric smearing.
- Traditionally, relatively long exposures have been chosen for Venus night-side imaging, typically picking values in the range 100msecs to 250msecs to minimise read noise[6]. 25msec would have been regarded as too short. However, as the previous section explains, read noise is actually much less of an issue for night-side imaging with modern cameras and this means that actually 25msec works fine as a exposure time for night-side imaging (at f4.5).
- For the Registax wavelet settings used, the bloated dayside crescent for the 225msec image at gain 260 (top row RH end) hides a very similar amount of the night-side region as does the wavelet-induced dark band around the dayside crescent for the 25msec image at gain 260 (top row LH end). In this set the same amount of night-side is seen in all, despite the 9x difference in exposure time and a correspondingly big difference in degree of over-exposed dayside bloating.
- For the wavelet settings used, the dayside of the 225msec image at gain 180 (bottom row RH end) is identically sized and hides a similar amount of the night-side as in the 25msec gain 370 image (bottom row LH end). This is not surprising given the dayside is over-exposed to the same extent in both images, as gain and exposure are traded against each other.

Is 12-bit imaging a necessity, or is 8-bit sufficient?

In planetary imaging, most imaging is done with video frames having an 8-bit depth, with 256 possible grey levels. When enough of these 8-bit frames are stacked in a program like AutoStakkert! the inherent random variation in the signal from one frame to the next allows the stacking program to create a smooth 16-bit stacked image with ~65,000 possible grey levels in it.

Camera control software used by planetary imagers usually has a 16-bit mode as well as the normal 8-bit mode that can be selected by the user. Enabling the 16-bit mode doubles the amount of data from each frame, increasing HDD/SDD storage requirements, and can also throttle back the fps if the data transfer rate is too high. For Venus night-side imaging, should we use this higher bit depth mode, despite these possible disadvantages?

[6] For given optical set-up, the SNR due to **Shot Noise** in the stacked image is just dependent on the *total accumulated exposure time in the stack*, not the frame exposure time. Halving the frame exposure time gives twice as many frames for a fixed video length and the √2 worse SNR of the individual frames is exactly cancelled out by the √2 improved averaging from the extra frames you get. This means that for shot noise you can have higher gain and shorter exposure or lower gain and longer exposure and the shot noise in the final stack will be the same. **Read Noise,** however**,** has a different dependency with exposure as shorter exposure times increase the read noise in the stack. Here halving the frame exposure time halves the frame SNR. This is because it halves the signal but the magnitude of the frame read noise stays unchanged. This contrasts with shot noise where the shot noise is root of the signal - thus as the signal goes down, the shot noise drops too. For read noise this means that although you get 2x more frames, the √2 improvement that this brings does not make up for the 2x worse SNR of the individual frames. Overall it means that if read noise is significant, in order to minimise read noise it is best to maximise frame exposure time. These concepts are of key importance in Deep Sky imaging

16-bit imaging really means using the full 12-bits of the sensor's internal ADC. To the (low) end of this 12-bit string, the camera software adds four 0s, making a sort of hybrid 16-bit string but with a maximum of 4096 possible grey levels (instead of the ~65,000 you would get with a 'proper' 16-bit string). The conversion of the 12-bit string to a 16-bit string makes it much easier for a computer to handle the data which is configured around 8-bit multiples.

16-bit mode is really 12-bit in terms of bit depth and for the rest of this section I will for clarity refer to this mode as 12-bit - to differentiate it from the more normal 16-bit images that come from stacking. Again I mention that when enough 12-bit frames are stacked in a program like AutoStakkert! the variation in the signal allows the program to create a 'proper', smooth, 16-bit stacked images, with 16x the number of grey levels.

If we rejig our data in Table 1 to just look at the grey levels for the night-side signal and the total magnitude of the noise, we can see if it is better to choose the 12-bit mode over the more normal 8-bit mode.

Date	Time	Solar Altitude	Camera Exposure Gain	Frame NS signal in GLs of 4096	Frame 8-bit NS signal in GLs of 256	Frame total noise in GLs of 4096	Frame 8-bit noise GLs of 256	Frame SNR	Stack SNR
05/09/2023	04:42	-5.6°	75msec G300	13	0.8	23	1.5	0.5	20.3
05/09/2023	04:46	-5.0°	75msec G300	13	0.8	27	1.7	0.5	17.5
05/09/2023	04:52	-4.2°	100msec G300	17	1.1	43	2.7	0.4	12.8
05/09/2023	04:56	-3.6°	100msec G300	17	1.1	65	4.0	0.3	8.5
05/09/2023	05:08	-1.8°	100msec G240	8	0.5	55	3.5	0.2	5.0
15/09/2023	04:46	-7.6°	75msec G260	5	0.3	15	0.9	0.4	13.3
23/09/2023	04:35	-11.3°	25msec G260	2	0.1	12	0.8	0.2	9.9
23/09/2023	04:33	-11.6°	75msec G260	5	0.3	19	1.2	0.3	10.2
23/09/2023	04:37	-11.0°	225msec G260	16	1.0	34	2.1	0.5	10.1
23/09/2023	04:43	-10.1°	25msec G370	6	0.4	40	2.5	0.2	10.1
23/09/2023	04:46	-9.6°	75msec G275	6	0.4	23	1.5	0.3	10.0
23/09/2023	04:40	-10.5°	225msec G180	6	0.4	15	0.9	0.4	9.0

Table 2. Signal and total noise. 12-bit versus 8-bit comparison of total grey levels

In the first grey column, you can see the number of grey levels for the night-side signal for the 12-bit frames in the different chosen videos. It varies from 2 to 17 grey levels. In the second grey column the magnitude of the noise in the frames is greater, at 12 to 65 grey levels. This high level of noise means there is more than enough random variation in the signal to smoothly render a 16-bit stacked image when the frames are stacked together in AutoStakkert!.

In the yellow columns I have divided the data in the grey columns by 16 to see how many grey levels of signal and how many grey levels of noise there would have been in the frames if the camera had been running in 8-bit mode instead of 12-bit mode. The magnitude of the signal now

averages between just 0.1 and 1.1 grey levels, whilst the magnitude of the noise is between 0.8 and 4 grey levels.

A frame signal which is so low as something like 0.1 grey levels is not a problem as long as there is enough variation in the signal to allow the stacking process to work correctly and convert the data to a smooth 16-bit image. If it can do this, the 0.1 grey level signal will end up as 26 grey levels in the 16-bit stacked image (256x higher). A more critical concern is whether 0.8 to 4 grey levels of noise is enough to make a smooth 16-bit image when stacked.

To answer this, we can turn to an interesting discussion involving Emil Kraaikamp, the author of AutoStakkert!: https://www.cloudynights.com/topic/330342-when-to-use-8-or-12-bit-a-small-analysis/#entry4237639. In this discussion, Emil calculates that if you have 2 grey levels of noise in a signal, the quantisation error between a (1000 frame) stacked image made up from 12-bit frames and one made up from 8-bit frames is just 1%. This difference rises to 4% for 1 grey level of noise and 15% for 0.5 bits of noise. Any less than 0.5 grey levels of noise and the error rises very rapidly.

This does indicate that with the range of camera settings used in my runs, there would have been just about enough random variation if I had used 8-bit mode to smoothly render a 16-bit stacked image without leading to significant quantisation errors (where the image would look posterised and not smoothly varying in brightness).

I do find this conclusion surprising, as previous to carrying out this analysis I did think that 12-bit imaging was an absolute necessity for Venus night-side imaging. At the next apparition in Feb. 2025 I plan on carrying out some experiments comparing 12-bit and 8-bit imaging. I am not recommending that imagers switch to 8-bit imaging given the potential dangers of quantisation errors, but 12-bit may be less vital than previously thought.

How short an exposure can be used on the Venus night-side?

Given the good 25msec processed images shown in figure 8, is there scope to further reduce the frame exposure time to help with the seeing at low altitude by reducing atmospheric smearing? This will be considered from two different perspectives:

- Quantisation Errors/Posterisation.
  In the Emil Kraaikamp discussion referenced in the previous section, the statement is made that if you have at least 2 grey levels of shot noise in the signal then the conversion to a 16-bit image by the stacking process is smooth with minimal quantisation errors. Given that in table 2, for an exposure time of 25msec and 12-bit imaging, there are 12 grey levels of noise at gain 260 (4:35UT on 23/9) and 40 levels at gain 370 (4:43UT on 23/9) it seems that there is a huge amount of headroom in noise levels to further reduce exposure without getting into quantisation errors and posterisation issues. This is all provided we do stick to12-bit imaging.

- Read Noise.
  In table 1 we see low levels of read noise in the stacked 25msec images, with it contributing just 2% to the total noise. If exposures are halved to 12.5msec we would expect read noise in the stack to increase by √2. Looking now at shot noise, as previously explained, provided

that we are not data rate limited (fps not throttled by high data loads) halving the exposure will have no effect on shot noise in the final stack. If shot noise in unchanged but read noise increases by √2, and as noise adds in quadrature, the contribution of the read noise to the total noise would effectively double from 2% to 4%, but still be very minor compared to the shot noise.

It seems there is enough of an argument to try exposures of the Venus night-side (at f4.5 and 12-bit) of significantly less than 25msec. In October 2023, experiments by Tom Williams shown that in good conditions the night-side can be made out with just a 1msec frame exposure (at f4.5) with 12-bit imaging. In Spring of 2025, the next night-side imaging opportunity, frame exposure times of 12.5msec and 6.25msec will be tried alongside 25msec to better understand the benefits and downsides of such short exposures.

Reducing SNR with Increasing Phase

You may have noticed in table 1 that for images taken in dark skies[7] there is a trend of falling SNR as the month progresses. Why is this?

The simple reason for this, is that as it is a morning apparition as the month progresses the dayside becomes larger in phase and at the same time the planet's angular size falls. The net result is that the angular distance between the dayside terminator and 31% reference position decreases significantly during the month, leading to more and more glare at this night-side location. As we have seen, for images taken in dark skies with the Sun more than 6° below the horizon, it is the dayside glare which is the major cause of shot noise and increasing glare leads to increased shot noise and results in falling SNR. On top of this increase in noise, the proportion of the disc which is night-side, as well as the angular size of the region, both decrease significantly from the start to the end of September. This progression significantly impacts image quality and the ability to image details in the night-side region.

What this all means for Imagers of the Night-side of Venus.

- To minimise noise due to twilight, image when the Sun is 6° or more below the horizon
- Image when the phase of dayside crescent is small and the planet large, to minimise glare which reduces the SNR of the night-side
- Don't worry about read noise when imaging with modern planetary cameras
- Use 12-bit imaging (although 8-bit might work okay too)
- It is worth trying exposures of 25msec (at f4.5 and 12-bit mode) or less to reduce atmospheric smearing effects and improve resolution

[7] All images on 23rd Sept have Sun at an altitude of less than -6° as does the image on 15th September. This means they are essentially taken in dark skies. The only image on 5th where the solar altitude is close to -6° is that taken at 04:42UT where the Sun was at -5.6°. Thus we are comparing the SNR of the 04:42UT image on the 5th September with the SNR of the image from 15th and all those taken on the 23rd.

Recent observations of Venus

The elongation has only recently just started and with the planet still low in the west at sunset, it is not surprising that only a few observations have been submitted so far:

Part One: Visual Observations

Paul G. Abel, Leicester UK:

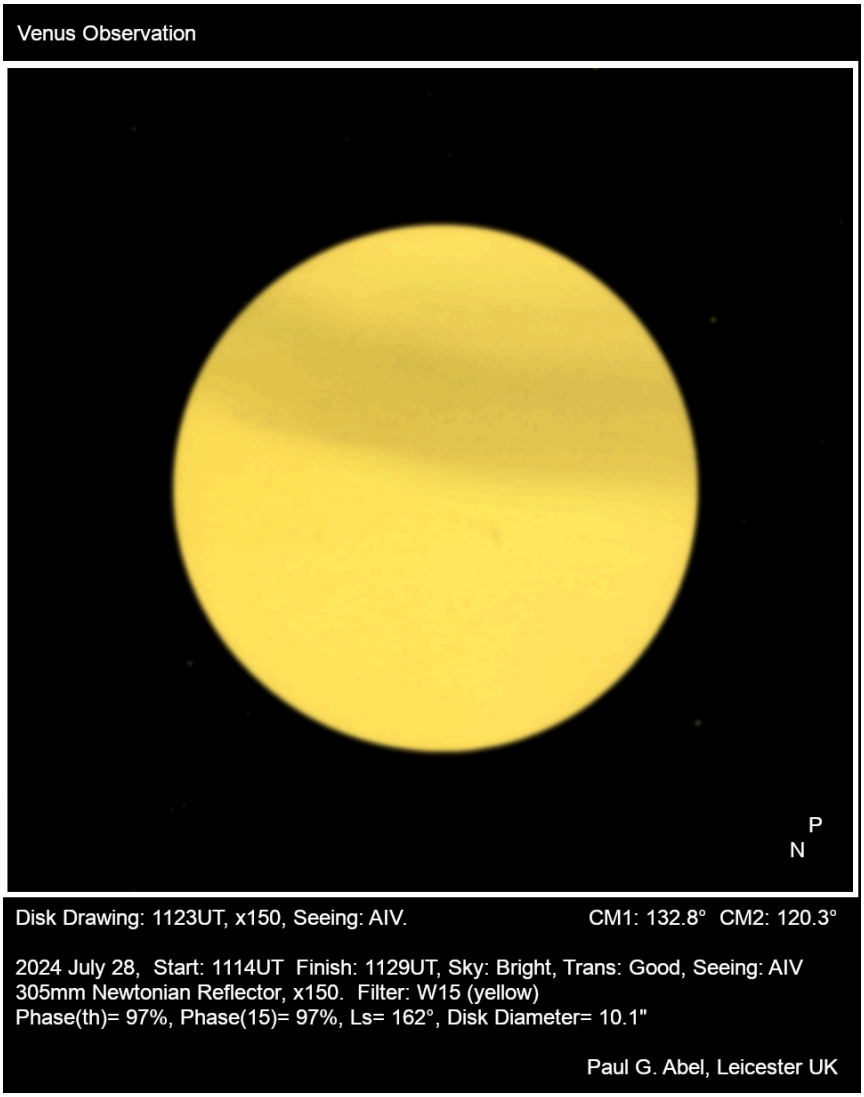

Part Two: Digital Observations

Antonio Cidadao, Portugal:

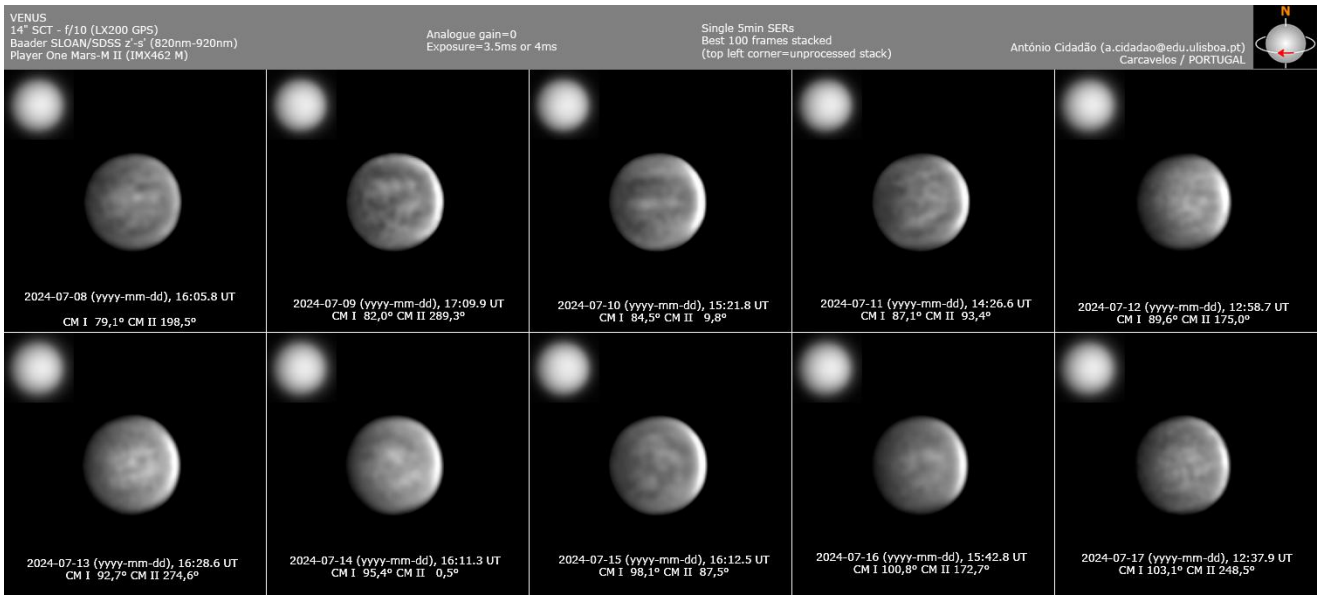

Luigi Morrone, Italy:

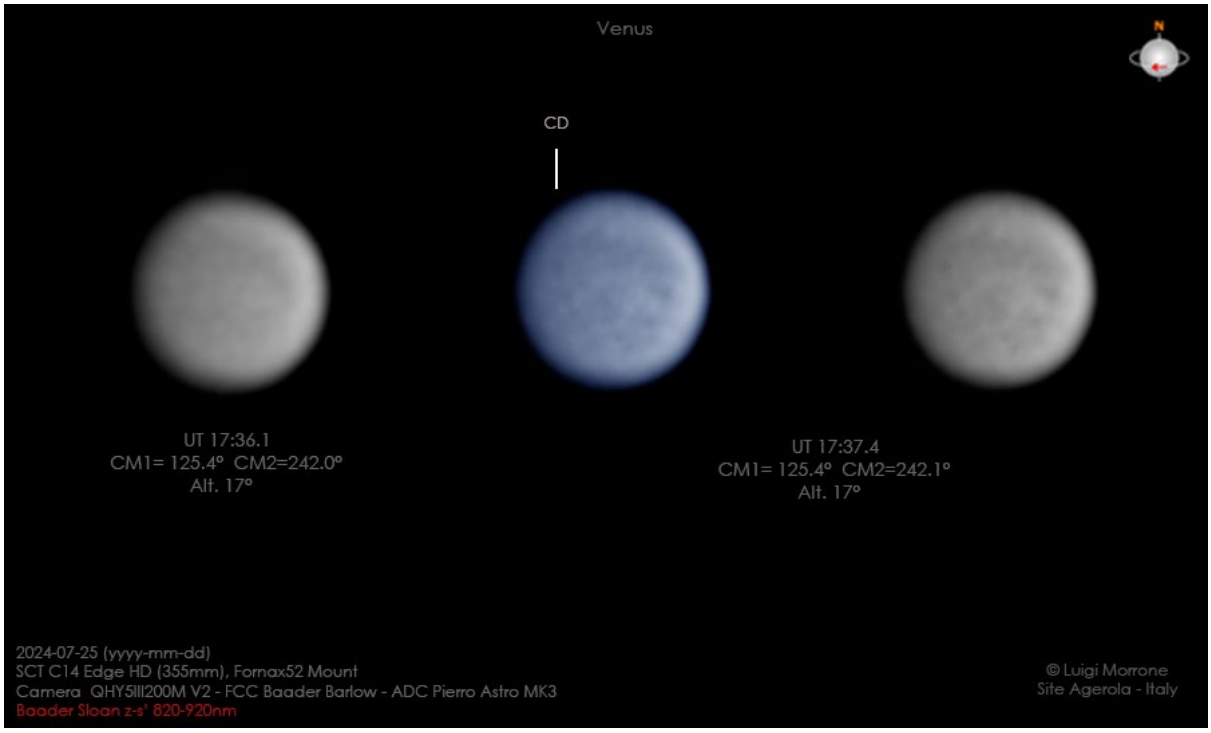

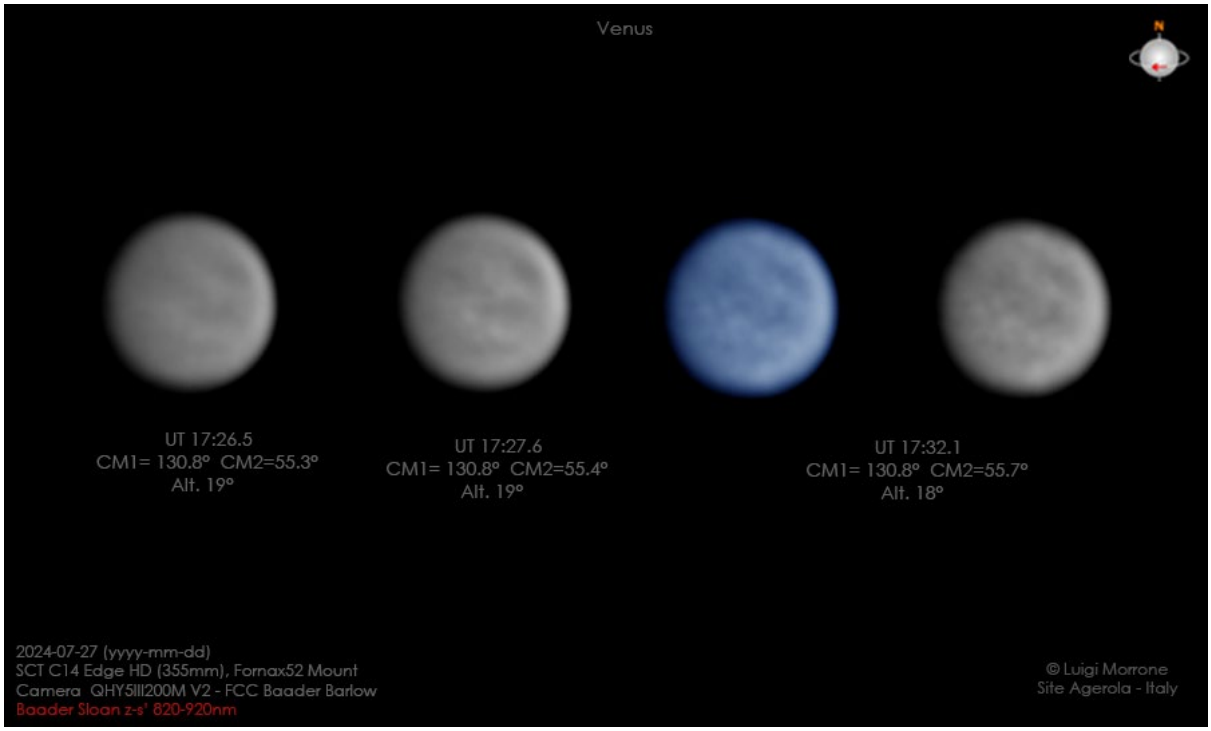
Venus
N
UT 17:26.5
CM1= 130.8° CM2=55.3°
Alt. 19°
UT 17:27.6
CM1= 130.8° CM2=55.4°
Alt. 19°
UT 17:32.1
CM1= 130.8° CM2=55.7°
Alt. 18°
2024-07-27 (yyyy-mm-dd)
SCT C14 Edge HD (355mm), Fornax52 Mount
Camera QHY5IIII200M V2 - FCC Baader Barlow
Baader Sloan z-s' 820-920nm
© Luigi Morrone
Site Agerola - Italy